Accepted version
Licence CC BY-NC-ND
Please cite as: Zengin G, Ferrante C, Senkardes I, Gevrenova R, Zheleva-Dimitrova D, Menghini L, Orlando G, Recinella L, Chiavaroli A, Leone S, Brunetti L, Picot-Allain CMN, Rengasamy KR, Mahomoodally MF. Multidirectional biological investigation and phytochemical profile of Rubus sanctus and Rubus ibericus. Food Chem Toxicol. 2019 May;127:237-250.
doi: 10.1016/j.fct.2019.03.041.

Multidirectional biological investigation and phytochemical profile of *Rubus sanctus* and *Rubus ibericus*

Gokhan Zengin[1*], Claudio Ferrante[2], Ismail Senkardes[3], Reneta Gevrenova[4], Dimitrina Zheleva-Dimitrova[4], Luigi Menghini[2], Giustino Orlando[2*], Lucia Recinella[2], Annalisa Chiavaroli[2], Sheila Leone[2], Luigi Brunetti[2], Carene Marie Nancy Picot-Allain[5], Kannan RR Rengasamy[6], Mohamad Fawzi Mahomoodally[5]

[1]*Department of Biology, Faculty of Science, Selcuk University, Konya, Turkey*
[2]*Department of Pharmacy, University "G. d'Annunzio" of Chieti-Pescara, Chieti 66100, Italy*
[3]*Department of Pharmaceutical Botany, Faculty of Pharmacy, Marmara University, Istanbul, Turkey*
[4] *Department of Pharmacognosy, Faculty of Pharmacy, Medical University of Sofia, Bulgaria*
[5]*Department of Health Sciences, Faculty of Science, University of Mauritius, 230 Réduit, Mauritius*
[6] *REEF Environmental Consultancy, #2 Kamaraj Street, S.P. Nagar, Puducherry 605 001, India,*

Corresponding Authors: gokhanzengin@selcuk.edu.tr (G. Zengin) and giustino.orlando@unich.it (G. Orlando)

Abstract

In the present study, the biological properties, including, the enzyme inhibitory and antioxidant activities, as well as, the phytochemical profile of the ethyl acetate, methanol, and water extracts of *Rubus sanctus* Schreb. and *Rubus ibericus* Juz. leaves were determined using *in vitro* bioassays. Wide range of phytochemicals, including, hydroxybenzoic acids, hydroxycinnamic acids, acylquinic acids, ellagitannins, flavonoids, and triterpenoid saponins were determined using UHPLC-ESI/HRMS technique. The ethyl acetate and methanol extracts of the studied *Rubus* species effectively inhibited acetyl and butyryl cholinesterase. On the other hand, *R. sanctus* water extract showed low inhibition against α-amylase and prominent inhibitory action against α-glucosidase. Data collected from this study reported the radical scavenging and reducing potential of the studied *Rubus* species. Investigation of the protective effects of the different extracts of *R. sanctus* and *R. ibericus* in experimental model of ulcerative colitis was performed. The extracts were also tested on spontaneous migration of human colon cancer cells (HCT116) in wound healing experimental paradigm. Only *R. sanctus* methanol extract inhibited spontaneous HCT116 migration in the wound healing test. Our results suggested that *R. sanctus* and *R. ibericus* may be potential candidates as sources of biologically-active compounds for the development of nutraceuticals, pharmaceuticals, and/or cosmetics.

Keywords: *Rubus*; LC-MS; toxicity; antioxidant; anti-inflammatory; wound healing

Introduction

The *Rubus* genus consists of 900 to 1000 species distributed worldwide (Ryu et al., 2018). Archaeologists found evidence of the use of *Rubus* dating around 8000 BCE, postulating that species of the *Rubus* genus have been long used as food and medicinal source (Hummer, 2010). Besides, ethnobotanical data substantiate the use of *Rubus* species for therapeutic applications by several cultures across the globe. For instance, the young shoots of the *Rubus* species were traditionally used to heal wounds, insect bites, and pimples (Süntar et al., 2011). The aerial part of *R. fruticosus* was used against cough, the fruit juice was recommended for colitis, the roots were used against diarrhea, chewing the leaves of *R. fruticosus* was recommended to relieve toothache, a tea prepared from the roots was used for labour pain, and a decoction prepared from *R. fruticosus* roots was used to treat dysentery (Verma et al., 2014). Australian aborigines have long consumed *Rubus* fruits to induce mild laxative effect (Bakar et al., 2016). Indeed, *Rubus* fruits have long been consumed worldwide, for their possible health benefits or simply because of their good taste (Lee et al., 2012). A herbal tea prepared from the decoction of *R. sanctus* roots was used to alleviate pain and against rheumatism (Süntar et al., 2011). The fruits of *R. sanctus* were used as a diuretic and against diarrhoea, haemorrhoids, diabetes mellitus, and rheumatism. *R. discolor* (synonym of *R. ibericus*) fruits, leaves, and roots were used to treat nephritis and prostatitis. Additionally, the leaves were used to heal wounds and treat diarrhoea (Veličković et al., 2016). In Traditional Chinese Medicine, a mixture containing *R. chingii* was used to manage infertility,

Commentato [MOU1]: https://doi.org/10.1016/j.hermed.2015.09.002

impotence, frequent urination, low backache, and poor sight (Bakar et al., 2016). *R. parvifolius* roots were widely used for the treatment of hepatitis, rheumatism, and abdominal pain caused by postpartum stasis (Xu et al., 2017). Traditionally, teas and alcoholic infusions prepared from the leaves, shoots, and fruits of *R. grandifolius* were used for the management of diabetes, as depurative, diuretic, and to treat sore throat (Spínola et al., 2019).

Rubus species are rich sources of bioactive compounds, possessing multiple biological properties. Several studies reported the biological activities of *Rubus* species. For instance, euscaphic acid, isolated from *R. rosifolius*, has been reported to show significant antioxidant activity. Ellagic acid, quercetin, and kaempferol, identified from *R. rosifolius* were related to the chemopreventive properties of the plant (Campbell et al., 2017). Phenolic rich extracts of *R. rosifolius* presented antimicrobial properties with anti-quorum sensing properties and antioxidant activity (Oliveira et al., 2016). Three compounds isolated from *R. idaeus* rhizome showed neuroprotective effects *in vitro* (Xu et al., 2017). *R. hirsutus* fruits showed high antioxidant activity (Fu et al., 2015). *R. grandifolius* extracts inhibited α-glucosidase, β-glucosidase, α-amylase, lipase, and aldose reductase (Spínola et al., 2019). *R. fairholmianus* methanol root extract effectively lowered cell viability, ATP proliferation, and increased LDH release from human breast cancer cells (George et al., 2017). Previously, Shin and colleagues (2014) demonstrated protective effects induced by *R. coreanus* in experimental model of ulcerative colitis. Akkol et al. (2015) demonstrated the inhibitory action of extracts of *R. sanctus* aerial parts on collagenase and elastase.

Based on the multiple biological activities of several Rubus species, this study was designed to assess the possible inhibitory action of *R. sanctus* and *R. ibericus* against key enzymes relevant to Alzheimer's disease (acetyl and butyryl cholinesterases), skin hyperpigmentation complications (tyrosinase), and diabetes type 2 (α-amylase, and α-glucosidase). Besides, as far as our literature review could ascertain, there has not been any

study on the inhibitory action of *R. sanctus* and *R. ibericus* on the selected enzymes. The antioxidant potential of the selected Rubus species was also evaluated. The phytochemical profiles of the ethyl acetate, methanol, and water extracts of *R. sanctus* and *R. ibericus* were determined by UHPLC-ESI/HRMS. The protective effects of *R. sanctus* and *R. ibericus* extracts, in an experimental model of ulcerative colitis, constituted of rat colon specimens challenged with lipopolysaccharide (LPS) *ex vivo*, was assessed. Finally, the chemopreventive effects of *R. sanctus* and *R. ibericus* extracts on human colon cancer (HCT116) cell migration and invasion capacities (wound healing test) were investigated.

2. Materials and Methods

2.1. Plant materials

The Rubus species were collected in Kastamonu-Turkey (*R. ibericus*: Hanönü village, between Yeniköy and Yılanlı, 619 m; *R. sanctus*: Hanönü village, center of Yılanlı, 1015 m) in June 2018. The taxonomical identification was performed by the botanist Dr. Ismail Senkardes (Marmara University, Faculty of Pharmacy, Pharmaceutical Botany, Istanbul) and a voucher specimen of each species was kept in the herbarium of Marmara University. The leaves were allowed to dry for 10 days at the room temperature. Then, these samples were pulverised with a laboratory mill.

2.2. Extraction

To prepare ethyl acetate and methanol extracts, the leaves samples (5g in 100 mL solvent) were stirred overnight (24 h) at room temperature and filtered. After filtration, the extracts were concentrated using a rotary evaporator under vacuum at 40 °C. Water extract was prepared by boiling 5 g of leaves samples in 100 mL water for 20 min. The mixture was then filtered and dried by using a lyophiliser. The extracts were stored at +4 °C until further analysis.

2.3. Quantification of phytochemicals

With reference to our previous studies (Uysal et al., 2017), the total amount of phenolics (TPC) (by standard Folin-Ciocalteu method) and flavonoids (TFC) (by aluminum chloride method) were determined. The final results were expressed as equivalents of standard compounds, i.e., gallic acid (mg GAE/g) and rutin (mg RE/g) for TPC and TFC, respectively.

2.4. Metabolite profiling by UHPLC-ESI/HRMS

The UHPLC-ESI/HRMS analyses were achieved on a Q Exactive Plus heated electrospray ionization (HESI-II) – high resolution mass spectrometer (HRMS) (ThermoFisher Scientific, Inc., Bremen, Germany) equipped with an ultra-high-performance liquid chromatography (UHPLC) system Dionex Ultimate 3000RSLC (ThermoFisher Scientific, Inc.) (Zengin et al., 2017). The analytical details were given in supplemental material.

2.5. Determination of antioxidant and enzyme inhibitory effects

The enzyme inhibitory activity of *R. ibericus* and *R. sanctus* extracts were tested against α-amylase, α-glucosidase, acetyl cholinesterase (AChE), butyryl cholinesterase (BChE), and tyrosinase. The procedures of these assays were reported in our earlier work (Uysal et al., 2017). The enzyme inhibitory effects were expressed as equivalents of acarbose (for α-amylase and α-glucosidase), galantamine (for AChE and BChE), and kojic acid (for tyrosinase).

Antioxidant capacity of *R. ibericus* and *R. sanctus* extracts were spectrophotometrically determined using different methods including phosphomolybdenum, radical scavenging assays (DPPH and ABTS), reducing potentials (FRAP and CUPRAC), and ferrous ion chelating. The results were expressed as trolox (mg TE/g) and ethylenediaminetetraacetic acid equivalents (mg EDTAE/g). The procedures of assays were reported in our earlier work (Uysal et al., 2017).

The results of antioxidant and enzyme inhibitory assays were statistically with one-way ANOVA (by Tukey's test, p <0.05). The statistical procedures were performed by SPPS v. 17.0. Multivariate analysis (Pearson Correlation, heat map and Sparse Partial Least Squares (sPLS-DA) analysis) were performed by using R software v. 3.5.1.

2.6. Biological assays

Artemia salina lethality bioassay

Artemia salina cysts were hatched in oxygenated artificial sea water (1g cysts/L). After 24 h, brine shrimp larvae were gently transferred with a pipette in 6 well plate containing 2 mL of *Rubus* extracts at different concentrations (0.1-20 mg/mL) in artificial sea water. Ten larvae per well were incubated at 25-28 °C for 24h. After 24 h the number of living napulii were counted under light microscope and compared to control untreated group. Results were expressed as percentage of mortality calculated as:

$$\frac{T-S}{T} x100,$$

where, T is the total number of incubated larvae and S is the number of survival napulii. Living nauplii were considered those exhibiting light activating movements during 10 seconds of observation. For each experimental condition two replicates per plate were performed and experimental triplicates were performed in separate plates.

In vitro studies

The HCT116 cell lines were cultured in DMEM (Euroclone) supplemented with 10% (v/v) heat-inactivated fetal bovine serum and 1.2% (v/v) penicillin G/streptomycin in 75 cm^2 tissue culture flask (n=5 individual culture flasks for each condition). The cultured cells were maintained in humidified incubator with 5% CO_2 at 37 °C.

For cell differentiation, HCT116 cell suspensions at a density of 1×10^6 cells/mL were treated with various concentrations (10, 50, and 100 ng/mL) of phorbol myristate acetate (PMA, Fluka) for 24 h or 48 h (induction phase). Thereafter, the PMA-treated cells were washed twice with ice-cold pH 7.4 phosphate buffer solution (PBS) to remove PMA and non-adherent cells, whereas the adherent cells were further maintained for 48 h (recovery phase). Morphology of cells was examined under an inverted phase-contrast microscope.

To assess the basal cytotoxicity of *R. sanctus* and *R. ibericus* extracts, a viability test was performed on 96 micro well plates, using 3-(4,5-dimethylthiazol-2-yl)-2,5-diphenyltetrazolium bromide (MTT) test. Cells were incubated with extracts (ranging in the concentration 10-1000 µg/mL) for 24 h. Aliquot of 10 µL of MTT (5 mg/mL) was added to each well and incubated for 3 h. The formazan dye formed was extracted with DMSO and absorbance was recorded as previously described (Menghini et al., 2018). Effects on cell viability were evaluated in comparison to untreated control group.

Finally, HCT116 cell line was exposed to Rubus extracts, in wound healing experimental paradigm. HCT116 cells (6×10^3 cells/well) were seeded on 6-well plastic plates. Cells monolayers were preliminarily treated with a proliferation inhibitor mitomycin C (Sigma-Aldrich, St. Louis, Missouri, USA) at the non-toxic concentration of 5 µM, in order to exclude the effect of cell proliferation. After 2 h on cells in the confluence interval 85-90%, a wound was generated by scratching the cell monolayer using a 0-200 µL pipette tip. The sample was washed twice with PBS to remove detached cells. Cells were incubated in serum free media supplemented with Rubus extracts at the non-toxic concentration of 100 µg/mL. Cell migration was visualised by capturing at least 3 microscope images/well at time 0, 24 and 48 h. An inverted light microscope Leika equipped with Nikon 5100 camera was used to capture image at 4x magnification. The quantification of scratch area with no cells was quantified using Image-J software (NIH). Using GraphPad software (version 6.0), mean data

253 at T0, 24 and 48 h were calculated for untreated control and *Rubus* extracts and expressed as
254 percentage variation with reference to relative 100% of at 0 h.

255 *Ex vivo* studies

256 Male adult Sprague-Dawley rats (200-250 g) were housed in Plexiglass cages (40 cm
257 × 25 cm × 15 cm), two rats per cage, in air-conditioned colony rooms (22 ± 1 °C; 60%
258 humidity), on a 12 h/12 h light/dark cycle (light phase: 07:00 - 19:00 h), with free access to
259 tap water and food, 24 h/day throughout the study, with no fasting periods. Rats were fed a
260 standard laboratory diet (3.5% fat, 63% carbohydrate, 14% protein, 19.5% other components
261 without caloric value; 3.20 kcal/g). Housing conditions and experimentation procedures were
262 strictly in accordance with the European Union ethical regulations on the care of animals for
263 scientific research.

264 The experiments were approved by Local Ethical Committee (University "G.
265 d'Annunzio" of Chieti-Pescara) and Italian Health Ministry (Italian Health Ministry
266 authorization N. F4738.N.XTQ, delivered on 11th November 2018). Rats were sacrificed by
267 CO_2 inhalation (100% CO_2 at a flow rate of 20% of the chamber volume per min) and colon
268 specimens were immediately collected and maintained in humidified incubator with 5% CO_2
269 at 37 °C for 4 h, in RPMI buffer with added bacterial LPS (10 µg/mL) (incubation period).

270 During the incubation period, tissues were treated with scalar sub-toxic concentrations
271 of *R. sanctus* and *R. ibericus* extracts (100 µg/mL). The activity of extracts was compared to
272 sulfasalazine (2 mg/mL), an anti-inflammatory reference drug. Tissue supernatants were
273 collected, and nitrite production was determined by mixing 50 µL of the assay buffer with
274 50 µL of Griess reagent (1.5% sulfanilamide in 1 M HCl plus 0.15% N-(1-naphthyl)
275 ethylenediamine dihydrochloride in distilled water, [v/v]). After 10 min incubation at room

temperature, the absorbance at 540 nm was determined and nitrite concentrations were calculated from a sodium nitrite standard curve.

On the other hand, individual colon specimens were dissected and subjected to extractive procedures to evaluate serotonin 5-hydroxytrptamine (5-HT) (ng/mg wet tissue) as previously reported (Brunetti et al., 2014; Ferrante et al., 2016). As regards to 5-HT analysis, tissues were homogenized in ice bath for 2 min with Potter-Elvehjem homogenizer in 1 mL of 0.05 N perchloric acid containing 0.004% sodium EDTA and 0.010% sodium bisulfite. Thereafter, samples were analyzed by HPLC coupled to electrochemical detection consisting of ESA Coulochem III detector equipped with ESA 5014B analytical cell.

Additionally, malondialdehyde (MDA) level was determined by the thiobarbituric acid reactive substances (TBARS) method (Mihara et al., 1980). Briefly, tissue specimens were added with 1% H_3PO_4 and 0.6% thiobarbituric acid, and then incubated at 96 °C for 20 min. Absorbance was recorded at 532 nm, and the MDA level was expressed as g/mL.

Besides, LDH activity was measured by evaluating the consumption of NADH in 20 mM HEPES-K^+ (pH 7.2), 0.05% bovine serum albumin, 20 µM NADH and 2 mM pyruvate using a microplate reader (excitation 340 nm, emission 460 nm) according to manufacturer's protocol (Sigma-Aldrich, St. Louis, Missouri, USA). Data were from triplicate test and expressed as relative variations compared to vehicle-treated cells (Menghini et al., 2018).

2.7. Statistical analysis

Statistical analysis was performed using GraphPad Prism version 5.01 for Windows (GraphPad Software, San Diego, CA). Means ± S.E.M. were determined for each experimental group and analyzed by one-way analysis of variance (ANOVA), followed by Newman-Keuls comparison multiple test. Statistical significance was considered as $p < 0.05$. Regarding the animals randomized for each experimental group, the number was calculated

on the basis of the "Resource Equation" N=(E+T)/T (10≤E≤20) (Charan and Kantharia, 2013), and in accordance with the guidelines suggested by the "National Centre for the Replacement, Refinement and Reduction of Animals in Research" (NC3RS) and reported on the following web site: https://www.nc3rs.org.uk/experimental-designstatistics. N is the number of animals per treated group. E represents the degrees of freedom of the analysis of variance (ANOVA). T is the number of treatments. Considering that E values should be between 10 and 20, the animal number N for *ex vivo* analysis was chosen in accordance to an E value of 20.

3. Results and discussion

Quantification of total bioactive components

The Folin-Ciocalteu and aluminum chloride assays are rapid and simple quantitative phytochemical analyses currently used for the detection of bioactive secondary metabolites, namely, phenolics and flavonoids. Phenolics, consisting of one or more aromatic rings linked hydroxyl groups, are the most abundant class of secondary metabolites, involved in the reproductive, growth, and defence mechanisms of plants (Huot et al., 2014). The total phenolic content of the studied extracts ranged between 17.22-152.55 mg GAE/g extract and *R. ibericus* water extract showed the highest total phenolic content (Table 1). Likewise, Veličković et al. (2016) also reported that the aqueous extracts of *R. ibericus* leaves contained highest phenolic content. Flavonoids are a subclass of phenolic compounds and are well known for their antioxidant properties (Chen et al., 2018). In the present study, the total flavonoid content of the studied extracts ranged between 25.70-40.52 mg RE/g extract and *R. ibericus* ethyl acetate extract showed the highest total flavonoid content. A group of authors studied the flavonoid content of *R. ibericus* leaves collected from different locations and

extracted the plant materials using different solvents. Flavonoid yield was higher when acetone was used as extraction solvent, the sample collected from the different regions showed distinct difference in flavonoid content (Veličković et al., 2016).

UHPLC-ESI/HRMS results

Based on the accurate mass measurements, MS/MS fragmentation patterns, relative abundance of the precursor and fragment ions, elemental compositions, monoisotopic peak profiles, as well as comparison with reference standards and literature data, a variety of *Rubus* compounds were identified or tentatively elucidated. For the majority of assayed compounds, the mass accuracy of $M-H]^-$ in MS/MS analyses was within a level of 5 ppm.

Hydroxybenzoic acids and hydroxycinnamic acids, and their derivatives

The total ion chromatograms for the tested extracts were given in supplementary material (Figure S1). Hydroxybenzoic acids **2**, **4** and **9**, and hydroxycinnamic acids **6**, **8** and **12** were identified on the basis of the retention times, accurate masses, fragmentation patterns and comparison with authentic standards (Table 2). Peaks **1** ($[M-H]^-$ at *m/z* 331.067) and **3** ($[M-H]^-$ at *m/z* 315.072) yielded abundant fragment ions at *m/z* 169.013 [gallic acid-H]$^-$ and 153.018 [protocatechuic acid-H]$^-$, respectively, indicating the loss of 162 Da. Thus **1** and **3** were identified as gallic acid-*O*-hexoside and protocatechuic acid *O*-hexoside, respectively. In the same way, **5** and **7** were tentatively identified as two isomers of caffeic acid-*O*-hexoside. MS/MS spectra of **10** ($[M-H]^-$ at *m/z* 503.155) and **11** ($[M-H]^-$ at *m/z* 504.123) were acquired (Table 2). The base peak at *m/z* 161.023 [caffeic acid-H-H_2O]$^-$ together with fragment ions at *m/z* 179.034 [caffeic acid-H]$^-$ and 135.044 [caffeic acid-H-CO_2]$^-$ allowed to identify caffeic acid derivatives. Fragmentation pattern of **10** displayed subsequent losses of hexose units at *m/z* 341.0902 [M-H-Hex]$^-$ and 323.079 [M-H-2Hex]$^-$, indicating caffeoyl-dihexoside.

Prominent ions at *m/z* 282.070 [M-H-caffeoyl-60]$^-$ (**11**), 252.060 ([M-H-caffeoyl-90]$^-$ and 222.049 ([M-H-caffeoyl-120]$^-$ were consistent with cross ring cleavages of the hexose unit $^{0,4}X^-$, $^{0,3}X^-$ and $^{0,2}X^-$, respectively. Thus, **11** was ascribed to dicaffeoyl-hexoside.

Ellagitannins and ellagic acid derivatives

The abundant peak **17** at *m/z* 300.999 ([M-H]$^-$) matched the standard reference ellagic acid. Ellagic acid-*O*-pentoside (**15**) and ellagic acid-*O*-deohyhexoside (**16**) were identified based on the prominent ion at *m/z* 300.999 and matching MS/MS fingerprint as **17**, and data published by (Oszmiański et al., 2015). Concerning compound **14** ([M-H]$^-$at *m/z* 934.073), the loss of a hexahydroxydiphenoyl (HHDP) moiety (301 Da) at *m/z* 633.073 and a base peak at *m/z* 300.999 [ellagic acid-H]$^-$, along with fragment ions at *m/z* 257.009 [ellagic acid-H-CO_2]$^-$, 245.009 [ellagic acid-H-2CO]$^-$, 229.014 [ellagic acid-H-CO-CO_2]$^-$ and 217.014 [ellagic acid-H-3CO]$^-$, highlighted the presence of galloyl-bis-HHDP-hexoside. This compound could be related to the ellagitannins casuarictin/potentillin, previously reported in Rubus species (Donno et al., 2013; Oszmiański et al., 2015). Peak **13** ([M-H]$^-$ at *m/z* 1401.597) afforded prominent ions at *m/z* 633.0735 and 300.999 corresponding to galloyl-HHDP-hexose and ellagic acid, respectively. This fragmentation pattern could be tentatively assigned to lambertianin C (Oszmiański et al., 2015).

Acylquinic acids

Eighteen acylquinic acids were identified in the majority of the tested Rubus extracts (Table 2). Herein, the hydroxycinnamic acids are mainly linked to quinic acid. The assignment of the different acylquinic acids was based on the hierarchical key developed by Clifford and colleagues (Clifford et al., 2003; Clifford et al., 2005). Peaks **18**, **20** and **21** were identified as 3-*O*-, 5-*O*- and 4-*O*-caffeoylquinic acids ([M-H]$^-$at *m/z* 353.088), respectively,

according to the relative abundance of the characteristic fragment ions at *m/z* 191.055 [quinic acid-H]$^-$, 179.034 [caffeic acid-H]$^-$ and 173.045 [quinic acid-H-H_2O]$^-$ and 135.044 [caffeic acid-H-CO_2]$^-$ (Clifford et al., 2003; Clifford et al., 2005). Based on comparison with authentic standards, compounds **18** and **20** were identified as neochlorogenic and chlorogenic acid, respectively. In the same manner, peaks **19**, **24** and **25** were ascribed to 3-*O*-, 4-*O*- and 5-*O*-*p*-coumaroylquinic acids ([M-H]$^-$at *m/z* 337.093), while peaks **23**, **26** and **27** ([M-H]$^-$at *m/z* 367.103) were assigned as 1-*O*-, 4-*O*- and 5-*O*-feruloylquinic acid (Table 2). Among the diacylquinic acids, peaks **28**, **29** and **30** were related to 3,4-*O*-, 3,5-*O* and 4,5-*O*-dicaffeoylquinic acids ([M-H]$^-$at *m/z* 515.120); **28** and **30** yielded indicative fragment ions at 173.045 together with 353.088 ([M-H-caffeoyl]$^-$, while the presence of **29** was evidenced by the relative abundance of the ions at 191, 179 and 135 (Clifford et al., 2003; Clifford et al., 2005; Zheleva-Dimitrova et al., 2017). Compounds **31**-**34**, [M-H]$^-$at *m/z* 529.136 related to caffeoylferuloylquinic acid (Clifford et al., 2003; Clifford et al., 2005). Furthermore, **31** and **34** were discernible by the base peaks at *m/z* 193.050 [ferulic acid-H]$^-$ and 135.044 [caffeic acid-H-CO_2]$^-$, respectively. The formation of the abundant fragment ion at *m/z* 367.104 [M-H-caffeoyl]$^-$ (86.1%) (**31**) was favored for 3-feruloyl-5-caffeoylquinic acid, while 3-caffeoyl-5-feruloylquinic acid was witnessed by the abundant ions at 179.034 [caffeic acid-H]$^-$ (62.8%) (**34**) together with 161.023 [caffeic acid-H-H_2O]$^-$ (53.8%). Typical ions of 4-feruloyl-5-caffeoylquinic acid (**32**) fragmentation were observed at *m/z* 173.045 (base peak), 367.103 (64.4%) and 193.050 (17.9%). By comparison with 1,5-dicaffeoylquinic acid (Clifford et al., 2005; Clifford et al., 2007), **33** was assigned to 1-caffeoyl-5-feruloylquinic acid, evidenced by the fragment ions at *m/z* 161.023 (base peak) and 367.103 (20.3%).

Flavonoids

Five flavonoid aglycones **53**-**57** were tentatively identified in the studied extracts (Table 2). Regarding **53**, typical neutral losses of the flavonoid aglycones were observed at

m/z 245.082 $[M-H-CO_2]^-$, 205.051 $[M-H-3CO]^-$, 203.070 $[M-H-C_3O_2-H_2O]^-$. Fragment ions at *m/z* 163.038 ($^{1,4}B^-$), 137.023 ($^{1,3}A^-$) and 121.028 ($^{1,2}B^-$) were attributed to the Retro-Diels Alder (RDA) cleavages of the flavonoid skeleton (de Rijke et al., 2006). Consequently, **53** was identified as epicatechin. Indeed, the most important fragmentation pattern for **54** (luteolin) is the RDA cleavage which afforded ions at *m/z* 133.028 ($^{1,3}B^-$), 151.003 ($^{1,3}A^-$) and 107.012 ($^{0,4}A^-$). Fragments at *m/z* 241.050 $[M-H-CO_2]^-$ and 201.018 $[M-H-3CO]^-$ had low abundance (below 1%) which is consistent with the previous study (Zheleva-Dimitrova et al., 2018). Regarding **55** (quercetin), the precursor ion at 301.036 gave a series of neutral losses at *m/z* 273.041 $[M-H-CO]^-$, 255.030 $[M-H-2CO]^-$, 229.050 $[M-H-CO-CO_2]^-$. RDA cleavage generated $^{1,3}A^-$ at *m/z* 151.003, $^{0,2}A^-$ at *m/z* 163.003, $^{1,2}A^-$ at *m/z* 178.998, $^{1,2}B^-$ at *m/z* 121.0287 and $^{0,4}A^-$ at *m/z* 107.012 (Table 2). It is worth noting that **57** (isorhamnetin) yielded fragment ion at *m/z* 301.031 $[M-H-CH_3]^-$ together with radical aglycone $[M-H-CH_3]^{-\bullet}$ at *m/z* 300.028 (base peak) as has been seen previously (Cuyckens and Claeys, 2004). The identification of aforementioned flavonoid aglycones was confirmed by comparison with authentic standards.

Three isobaric flavonoids **36**-**38** shared the same $[M-H]^-$ at *m/z* 609.146 (exact mass). The MS/MS spectra of **36** and **37** showed losses of two hexose units yielding aglycone at *m/z* 285.041. Concerning **37**, RDA cleavage $^{0,2}A^-$ at *m/z* 163.003 and $^{1,3}A^-$ at *m/z* 151.003 suggested flavonol kaempferol, supported by abundant fragment ions at *m/z* 255. 030 ($-CH_2O$) (51.8%) and 227.035 ($-CH_2O-CO$) (34.2%). The aglycone of **36** was consistent with luteolin, witnessed by $^{1,3}B^-$ at 133. 028. Consequently, **36** and **37** were tentatively identified as luteolin-*O*- and kaempferol-*O*-dihexoside, respectively. Compounds **38**, **39**, **41**, **42** and **44** afforded the same abundant ion at *m/z* 301.035(6) $[quercetin-H]^-$ supported by the radical aglycone at *m/z* 300.027(8) as was seen previously for the quercetin-3-*O*-glycosides (Cuyckens and Claeys, 2004). Based on fragmentation pattern and comparison with authentic standards, **38**, **39** and

42 were identified as rutin, hyperoside and isoquercitrin, respectively, while **41** and **44** were assigned to quercetin-*O*-glucuronide and quercetin-*O*-pentoside, respectively.

The fragmentation fingerprints of **40**, **45**, **48**, **49**, **51** and **52** were associated with kaempferol derivatives, witnessed by the abundant fragment ion at *m/z* 285.040 supported by the ions at *m/z* 255, 227, 211, 179, 163, 151, 135 and 107 (**40**). The fragmentation of $[M-H]^-$ at *m/z* 579.136 (**40**) yielded low abundant ions at *m/z* 429.083 $[M-H-132-H_2O]^-$, 327.050 $[M-H-132-120]^-$ and 309.041 $[M-H-120-132-H_2O]^-$ indicating the presence of hexose and pentose moieties. The loss of 150 Da (132+120) suggested that latter could be linked to the hydroxyl group of the primary hexose. Moreover, the ion at *m/z* 309 indicated that the pentose unit is linked at position 2", since the fragment 120 Da ($^{0,2}X_0^-$) implies 3", 4", 5"and 6" (Ferreres et al., 2007). The presence of the radical aglycone at *m/z* 284.033 (base peak) was in agreement with 3-*O*-glycosidic bond of the primary hexose (Cuyckens and Claeys, 2004). Thus, **40** was tentatively identified as kaempferol-2"-*O*-pentosyl-3-*O*-hexoside. The fragmentation pathway of **51** and **52** involved consequent losses of caffeoyl and *p*-coumaroyl residue, respectively, at *m/z* 447.094, and hexose at *m/z* 285.041.

The caffeoyl residue (**51**) was evidenced by the prominent ions at *m/z* 179, 161 and 135, as was seen in caffeoylquinic acids (Table 2). Accordingly, **51** was assigned to kaempfero-*O*-caffeoylhexoside. Based on comparison with authentic standard, **52** was identified as kaempferol-3-*O*-(6-*p*-coumaroyl)-glucoside (tiliroside), commonly found in Rubus sp. (Gevrenova et al., 2013; Han et al., 2012). In the same way, retention times, fragmentation patterns and monoisotopic profiles of **45**, **47**, **49** and **50** were in good agreement with those of the reference standards kaempferol-3-*O*-rutinoside, isorhamnetin-3-*O*-glucoside, kaempferol-3-*O*-glucoside and luteolin-7-*O*-glucoside.

Triterpenoid saponins

MS/MS spectra of three isobaric pairs **59**/**61**, **60**/**62** and **63**/**64** were acquired (Table 2). Concerning **59**/**61**, the loss of a hexose unit afforded a fragment ion at *m/z* 517.317 corresponding to the [sapogenin-H]$^-$ which was consistent with a molecular formula $C_{30}H_{45}O_7$ (0.558 ppm). Its fragmentation pathway involved losses of 18 Da (H_2O) and 44 Da (CO_2), together with the concomitant losses of (H_2O+CO_2) at *m/z* 455.317, ($2H_2O$+CO_2) at *m/z* 437.305 and ($2H_2O$+$2CO_2$) at *m/z* 393.380, suggesting triterpenoid acid with at least two tertiary hydroxyl groups (Sandjo et al., 2017). This conclusion was consistent with barrinic acid-hexoside previously identified in the roots of *Rubus ctaraegifolia* (Jung et al., 2001). Formate adducts [M+HCO_2]$^-$ were observed at *m/z* 709.381 (**60**/**62**) and 695.402 (**63**/**64**). Their sapogenins were ascribed to the hydroxygypsogenin and arjunolic acid, respectively (Jung et al., 2001). In addition, ilexosapogenin A-hexoside was evidenced as main triterpenoid saponins in all studied extracts (Table 2) (Jung et al., 2001). Barrinic acid (**66**) was the dominant compound in both ethyl acetate extracts together with the abundant sapogenins ilexosapogenin A (**65**), arjunolic acid (**67**) and hydroxygypsogenic acid (**68**) (Table 2).

Antioxidant capacity

To determine the antioxidant properties of the different extracts of *R. sanctus* and *R. ibericus*, several antioxidant assays were employed. The total antioxidant capacity of the extracts, measured using the phosphomolybdenum assay, followed this order water > methanol > ethyl acetate extracts. It is worth mentioning that the total antioxidant capacity corresponded with total phenolic determinations. Indeed, several reports have demonstrated the relationship between phenolic content and antioxidant activity (Amzad Hossain and Shah, 2015; Encarnação et al., 2016). The anti-radical activity of the extracts was assessed using the DPPH and ABTS assays. In general, the methanol and water extracts of the studied *Rubus* species showed good anti-radical activities. Free radicals, being unstable and highly reactive,

475 are capable of damaging biological molecules leading to cell damage and homeostatic
476 disruption (Lobo et al., 2010). Multiple lines of evidence support the free radical scavenging
477 properties of several species of the *Rubus* genus (Bhandary et al., 2012; Ding, 2011;
478 Venskutonis et al., 2007). Upon evaluation of the reducing activity of the different extracts of
479 *R. sanctus* and *R. ibericus*, the water extracts of both *Rubus* species showed highest reducing
480 potential against FRAP and CUPRAC (Table 3). It is worth mentioning that *R. ibericus*
481 showed higher activity compared to *R. sanctus*. This finding is in line with Veličković et al.
482 (2016) who reported that higher reducing activity of *R. ibericus* aqueous leaves extract in the
483 FRAP assay. Besides, rutin, previously identified from the aqueous extract of *R. ibericus*
484 leaves (Keser et al., 2015) and known to possess potent reducing action (Apak et al., 2008)
485 might be responsible for the observed activity. The chelating potential of the different extracts
486 of the studied Rubus species was also investigated. According to data presented in Table 3,
487 the water extracts (52.20 and 59.83 mg EDTAE/g extract, for *R. sanctus* and *R. ibericus*,
488 respectively) of both Rubus species showed higher chelating activity.
489
490 ***Enzyme inhibitory properties***
491 We investigated the inhibitory activities of the ethyl acetate, methanol, and water
492 extracts of *R. sanctus* and *R. ibericus* against enzymes related to Alzheimer's disease, skin
493 hyperpigmentation complications, and diabetes type 2. As shown in Table 4, the ethyl acetate
494 and methanol extracts inhibited both acetyl and butyryl cholinesterase. The development of
495 cholinesterase inhibitors is still the most popular clinical strategy targeted for the management
496 of Alzheimer's disease. In fact, in the brain of Alzheimer's disease patients, the abnormal low
497 level of acetylcholine has been related to pathological features of Alzheimer's disease,
498 particularly cognitive decline (Li et al., 2018). *R. coreanus* ethanol extract showed inhibitory

activity against acetylcholinesterase *in vitro* and exerted memory ameliorating effects *in vivo* (Kim et al., 2013).

The ability of the extracts to inhibit tyrosinase was also established. In general, the ethyl acetate (121.55 and 124.28 mg KAE/g extract, for *R. sanctus* and *R. ibericus*, respectively) and methanol (131.44 and 132.05 mg KAE/g extract, for *R. sanctus* and *R. ibericus*, respectively) extracts of the studied Rubus species showed potent inhibitory action against tyrosinase. Plant extracts showing inhibitory activity towards skin-regulating enzymes, such as tyrosinase, are considered as promising candidates for the development of dermatological treatments and cosmetics as skin-whitening agents (Papaioanou et al., 2018).

In the present study, we assessed the ability of *R. sanctus* and *R. ibericus* extracts to inhibit the activity of α-amylase and α-glucosidase. The inhibition of carbohydrate hydrolysing enzymes is considered as an interesting therapeutic strategy to control glycaemic level (Zengin et al., 2018). However, it is worth mentioning that the excessive inhibition of α-amylase has been associated to a number of gastrointestinal complications caused by undigested food (Uysal et al., 2018). Thus, developing hypoglycaemic agents showing mild or no α-amylase inhibition and potent α-glucosidase inhibitory action is considered as the ideal therapeutic approach to the management of diabetes type 2. In the present study, *R. sanctus* water extract showed low inhibition against α-amylase (0.12 mmol ACAE/g extract) and prominent inhibitory action against α-glucosidase (24.85 mmol ACAE/g extract). Data collected from this study support the traditional use of *R. sanctus* leaves for the treatment of diabetes type 2 (Süntar et al., 2011).

We performed further statistical analysis to understand any relationship between total bioactive components and biological activities. As presented in Fig. 1, we observed strong correlation between total phenolic and antioxidant properties. It might be suggested that phenolics in the tested extracts were responsible for the observed antioxidant activities.

524 However, weak correlation was noted between phenolics and enzyme inhibitory effects. In
525 this sense, non-phenolic inhibitors could be attributed to observed enzyme inhibitory effects.
526 Apparently, the extracts were divided depending on species in sPLS-DA analysis. Also, VIP
527 values are higher than 1 for total flavonoid content, phosphomolybdenum and metal chelating
528 assays, which are main parameters to divide the extracts as well as species.
529
530 ***Biological assays***
531 As a preliminary approach to evaluate potential toxicity, the ethyl acetate, methanol,
532 and water of the selected Rubus species, (0.1-100 mg/mL) were tested on brine shrimp
533 lethality assay. *Artemia salina* Leach is commonly used to investigate toxicological activities
534 of plant extracts (Ohikhena et al., 2016). The evaluation of *Rubus* extract toxicity revealed
535 LC_{50} values in the range 2.52-5.12 mg/mL.
536 Based on LC_{50} values recorded, a concentration of 500 µg/mL was chosen for
537 subsequent assessment on human colon cancer-derived HCT116 cell using the MTT test. The
538 tested extracts (10-500 µg/mL) confirmed a good biocompatibility, as revealed by the null
539 effect on cell line viability in the range (10-100 µg/mL). On the other hand, at the highest
540 tested concentration (500 µg/mL) cell viability decreased under the limit of biocompatibility
541 (viability ≥ 70%).
542 Furthermore, the effect of *Rubus* extracts on spontaneous HCT116 cell migration, up
543 to 48 h after scratching stimulus, was assessed. Results revealed that most of the extracts were
544 ineffective in modulating spontaneous HCT116 cell migration. By contrast, *R. sanctus*
545 methanol extract significantly inhibited spontaneous cell migration thus suggesting a potential
546 protective effect against migration and invasion capacities of HCT116 human colon cancer
547 cells (Figure 2).

548 A subsequent panel of experiments was performed on isolated rat colon specimens
549 challenged with LPS, a validated *ex vivo* experimental paradigm to evaluate the efficacy of
550 drugs and extracts on oxidative and inflammatory pathways involved in ulcerative colitis
551 (Locatelli et al., 2017; Menghini et al., 2016; Menghini et al., 2018). Overproduction of
552 reactive oxygen/nitrogen species (ROS/RNS) has long been considered to play a key in tissue
553 damage through disruptive peroxidation reactions on macromolecules, including proteins,
554 lipids, and nucleic acids (Uttara et al., 2009). Particularly, lipid peroxidation has been long
555 involved in tissue chronic inflammatory diseases (Achitei et al., 2013). The role of ROS/RNS,
556 mainly synthesized by activated macrophages and neutrophils, include neutrophils recruitment
557 at the inflamed tissues (Fialkow et al., 2007; Kruidenier and Verspaget, 2002). To this regard,
558 the assessment of tissue nitrite level is a useful marker of nitric oxide (NO) synthesis, which is
559 an indicator of disease activity in ulcerative colitis (Goggins et al., 2001). NO is a free radical
560 which can react with multiple tissue biomolecules, thus giving oxidation products including
561 nitrite, nitrate, nitrosyl (NO-heme) species, and S- and N-nitroso products. The level of these
562 NO-related products reflects the nitrosative stress due to inflammation-induced upregulation
563 of the inducible NO synthase (iNOS) (Saijo et al., 2010)
564 *R. sanctus* methanol and ethyl acetate extracts were equally able to reduce LPS-
565 induced nitrite level in isolated colon (Figure 3), while sulfasalazine resulted ineffective in
566 downregulating nitrite levels. The null effect of sulfasalazine on nitrite level corroborates with
567 the recent findings by Cetin et al. (2017) which observed a null effect displayed by
568 sulfasalazine on nitrosative stress pathway, evaluated as nitrite level. *R. sanctus* methanol and
569 *R. ibericus* ethyl acetate extracts were also able to reduce colon MDA levels, upregulated by
570 LPS challenging (Figure 4). The extracts were as effective as sulfasalazine, which was able to
571 restore basal MDA level in isolated rat colon challenged with LPS, according to the recent
572 findings by Soliman et al. (2019). Consistent with the effect on MDA level, the extracts

reduced LDH level on rat colon, showing activity as effective as sulfasalazine (Figure 5). LDH could be considered a predictive marker of tissue damage, especially in the gut, and reduced LDH activity following extracts treatment was related to protective effects in IBDs (Kannan and Guruvayoorappan, 2013; Nagarjun et al., 2017). Actually, the downregulation of nitrite, MDA and LDH level induced by the extracts is consistent with their total phenol and flavonoid content (Raihan et al., 2009). The relative abundance in kaempferol could explain, albeit partially, the major blunting effect exerted by *R. sanctus* methanol on LPS-induced nitrite, MDA and LDH level, in isolated rat colon.

5-HT pro-inflammatory role in ulcerative colitis has been previously suggested (Regmi et al., 2014), possibly involving the activation of 5-HT3 receptors (Mousavizadeh et al., 2009). Previously, it was observed that antioxidant and anti-inflammatory chamomile and devil's claw extracts reduced 5-HT steady state level, in rat colon challenged with LPS (Menghini et al., 2016; Menghini et al., 2017). Several studies confirmed that steady state tissue 5-HT concentration also proved to be a valuable index of neurotransmitter activity, including synthesis and release (Bungo et al., 2009; Clark et al., 2006). Aqueous extracts from each species revealed equally effective in blunting LPS-induced 5-HT steady state levels, in rat colon (Figure 6). Additionally, *R. sanctus* ethyl acetate extract revealed to be more effective than sulfasalazine (Menghini et al., 2016). The inhibitory effects exerted by *R. sanctus* and *R. ibericus* extracts could be related to multiple concomitant mechanisms. On one side, the phenol and flavonoid content could reduce 5-HT level as a result of the antioxidant activity. On the other side, the possible inhibitory effect on 5-HT activity induced by multiple components of flavonoid fraction which could reduce 5-HT release and antagonize pro-inflammatory 5-HT3 mediated-pathway (Chen et al., 2002; Herbrechter et al., 2015).

Conclusion

Results of the present investigation revealed the potential of the selected *Rubus* species as effective enzyme inhibitors and antioxidant agents. Besides, findings of this study highlight the importance of solvent choice in the extraction of bioactive compounds from plants. The water extracts showed high phenolic content and antioxidant activity while the ethyl acetate and methanol extracts of *R. sanctus* and *R. ibericus* showed potent enzyme inhibitory activity. In the quest for safer hypoglycaemic agents, *R. sanctus* water extract revealed to be a promising candidate, showing low α-amylase inhibition and prominent α-glucosidase inhibitory activity.

On the other hand, *R. sanctus* methanol extract showed anti-inflammatory activity in colon cells, showing significant blunting effects on LPS-induced levels of well-established markers of oxidative stress and tissue damage such as nitrites, MDA, and LDH. Besides, *R. sanctus* methanol extract displayed a significant inhibition of spontaneous migration of HCT116 cell line, thus suggesting a potential protective effect against migration and invasion capacities of human colon cancer cells. Further studies are warranted to isolate and characterize bioactive compounds present in the studied *Rubus* extracts for the development of novel nutraceuticals, pharmaceuticals and/or cosmetics.

Conflict of Interest

The authors declare that there are no conflicts of interest.

References

Achitei, D., Ciobica, A., Balan, G., Gologan, E., Stanciu, C., Stefanescu, G., 2013. Different profile of peripheral antioxidant enzymes and lipid peroxidation in active and non-active inflammatory bowel disease patients. Digestive diseases and sciences 58, 1244-1249.

Amzad Hossain, M., Shah, M.D., 2015. A study on the total phenols content and antioxidant activity of essential oil and different solvent extracts of endemic plant Merremia borneensis. Arabian Journal of Chemistry 8, 66-71.

628 Apak, R., Güclü, K., Özyürek, M., Celik, S.E., 2008. Mechanism of antioxidant capacity
629 assays and the CUPRAC (cupric ion reducing antioxidant capacity) assay.
630 Microchimica Acta 160, 413-419.
631 Bakar, A., Fadzelly, M., Ismail, N.A., Isha, A., Ling, M., Lee, A., 2016. Phytochemical
632 composition and biological activities of selected wild berries (Rubus moluccanus L.,
633 R. fraxinifolius Poir., and R. alpestris Blume). Evidence-Based Complementary and
634 Alternative Medicine 2016.
635 Bhandary, B., Lee, H.Y., Back, H.I., Park, S.H., Kim, M.G., Kwon, J.W., Song, J.Y., Lee,
636 H.K., Kim, H.R., Chae, S.W., Chae, H.J., 2012. Immature Rubus coreanus Shows a
637 Free Radical-Scavenging Effect and Inhibits Cholesterol Synthesis and Secretion in
638 Liver Cells. Indian journal of pharmaceutical sciences 74, 211-216.
639 Brunetti, L., Leone, S., Orlando, G., Ferrante, C., Recinella, L., Chiavaroli, A., Di Nisio, C.,
640 Shohreh, R., Manippa, F., Ricciuti, A., 2014. Hypotensive effects of omentin-1 related
641 to increased adiponectin and decreased interleukin-6 in intra-thoracic pericardial
642 adipose tissue. Pharmacological Reports 66, 991-995.
643 Bungo, T., Shiraishi, J.-i., Yanagita, K., Ohta, Y., Fujita, M., 2009. Effect of
644 nociceptin/orphanin FQ on feeding behavior and hypothalamic neuropeptide
645 expression in layer-type chicks. General and comparative endocrinology 163, 47-51.
646 Campbell, T.F., McKenzie, J., Murray, J., Delgoda, R., Bowen-Forbes, C.S., 2017. Rubus
647 rosifolius varieties as antioxidant and potential chemopreventive agents. Journal of
648 Functional Foods 37, 49-57.
649 Cetin, C., Erdogan, A.M., Dincel, G.C., Bakar, B., Kisa, U., 2017. Effects of sulphasalazine in
650 cerebral ischemia reperfusion injury in rat. Archives of medical research 48, 247-256.
651 Charan, J., Kantharia, N., 2013. How to calculate sample size in animal studies? Journal of
652 pharmacology & pharmacotherapeutics 4, 303.
653 Chen, W., Jin, M., Wu, W., 2002. Experimental study on inhibitory effect of rutin against
654 platelet activation induced by platelet activating factor in rabbits. Zhongguo Zhong xi
655 yi jie he za zhi Zhongguo Zhongxiyi jiehe zazhi= Chinese journal of integrated
656 traditional and Western medicine 22, 283-285.
657 Chen, X., Deng, Z., Zhang, C., Zheng, S., Pan, Y., Wang, H., Li, H., 2018. Is antioxidant
658 activity of flavonoids mainly through the hydrogen-atom transfer mechanism? Food
659 Research International.
660 Clark, K.A., MohanKumar, S.M., Kasturi, B.S., MohanKumar, P., 2006. Effects of central
661 and systemic administration of leptin on neurotransmitter concentrations in specific
662 areas of the hypothalamus. American Journal of Physiology-Regulatory, Integrative
663 and Comparative Physiology 290, R306-R312.
664 Clifford, M.N., Johnston, K.L., Knight, S., Kuhnert, N.J.J.o.a., chemistry, f., 2003.
665 Hierarchical scheme for LC-MS n identification of chlorogenic acids. 51, 2900-2911.
666 Clifford, M.N., Knight, S., Kuhnert, N.J.J.o.A., Chemistry, F., 2005. Discriminating between
667 the six isomers of dicaffeoylquinic acid by LC-MS n. 53, 3821-3832.
668 Clifford, M.N., Wu, W., Kirkpatrick, J., Kuhnert, N.J.J.o.A., Chemistry, F., 2007. Profiling
669 the chlorogenic acids and other caffeic acid derivatives of herbal Chrysanthemum by
670 LC− MS n. 55, 929-936.
671 Cuyckens, F., Claeys, M.J.J.o.M.s., 2004. Mass spectrometry in the structural analysis of
672 flavonoids. 39, 1-15.
673 de Rijke, E., Out, P., Niessen, W.M., Ariese, F., Gooijer, C., Udo, A.T.J.J.o.c.A., 2006.
674 Analytical separation and detection methods for flavonoids. 1112, 31-63.
675 Ding, H.Y., 2011. Extracts and constituents of Rubus chingii with 1,1-diphenyl-2-
676 picrylhydrazyl (DPPH) free radical scavenging activity. International journal of
677 molecular sciences 12, 3941-3949.

678 Donno, D., Cavanna, M., Beccaro, G.L., Mellano, M., Torello Marinoni, D., Cerutti, A.K.,
679 Bounous, G.J.J.o.A.B., Quality, F., 2013. Currants and strawberries as bioactive
680 compound sources: determination of antioxidant profi les with HPLC-DAD/MS. 86,
681 1-10.
682 Encarnação, S., de Mello-Sampayo, C., Graça, N.A.G., Catarino, L., da Silva, I.B.M., Lima,
683 B.S., Silva, O.M.D., 2016. Total phenolic content, antioxidant activity and pre-clinical
684 safety evaluation of an Anacardium occidentale stem bark Portuguese hypoglycemic
685 traditional herbal preparation. Industrial Crops and Products 82, 171-178.
686 Ferrante, C., Orlando, G., Recinella, L., Leone, S., Chiavaroli, A., Di Nisio, C., Shohreh, R.,
687 Manippa, F., Ricciuti, A., Vacca, M., 2016. Central inhibitory effects on feeding
688 induced by the adipo-myokine irisin. European journal of pharmacology 791, 389-394.
689 Ferreres, F., Gil-Izquierdo, Á., Andrade, P.B., Valentão, P., Tomás-Barberán, F.J.J.o.C.A.,
690 2007. Characterization of C-glycosyl flavones O-glycosylated by liquid
691 chromatography–tandem mass spectrometry. 1161, 214-223.
692 Fialkow, L., Wang, Y., Downey, G.P., 2007. Reactive oxygen and nitrogen species as
693 signaling molecules regulating neutrophil function. Free Radical Biology and
694 Medicine 42, 153-164.
695 Fu, Y., Zhou, X., Chen, S., Sun, Y., Shen, Y., Ye, X., 2015. Chemical composition and
696 antioxidant activity of Chinese wild raspberry (Rubus hirsutus Thunb.). LWT - Food
697 Science and Technology 60, 1262-1268.
698 George, B.P., Abrahamse, H., Hemmaragala, N.M., 2017. Phenolics from Rubus
699 fairholmianus induces cytotoxicity and apoptosis in human breast adenocarcinoma
700 cells. Chemico-Biological Interactions 275, 178-188.
701 Gevrenova, R., Badjakov, I., Nikolova, M., Doichinova, I.J.B.s., ecology, 2013. Phenolic
702 derivatives in raspberry (Rubus L.) germplasm collection in Bulgaria. 50, 419-427.
703 Goggins, M.G., Shah, S.A., Goh, J., Cherukuri, A., Weir, D.G., Kelleher, D., Mahmud, N.,
704 2001. Increased urinary nitrite, a marker of nitric oxide, in active inflammatory bowel
705 disease. Mediators of inflammation 10, 69-73.
706 Han, N., Gu, Y., Ye, C., Cao, Y., Liu, Z., Yin, J.J.F.c., 2012. Antithrombotic activity of
707 fractions and components obtained from raspberry leaves (Rubus chingii). 132, 181-
708 185.
709 Herbrechter, R., Ziemba, P.M., Hoffmann, K.M., Hatt, H., Werner, M., Gisselmann, G., 2015.
710 Identification of Glycyrrhiza as the rikkunshito constituent with the highest
711 antagonistic potential on heterologously expressed 5-HT3A receptors due to the action
712 of flavonoids. Frontiers in pharmacology 6, 130.
713 Hummer, K.E., 2010. Rubus pharmacology: antiquity to the present. HortScience 45, 1587-
714 1591.
715 Huot, B., Yao, J., Montgomery, B.L., He, S.Y., 2014. Growth–Defense Tradeoffs in Plants: A
716 Balancing Act to Optimize Fitness. Molecular Plant 7, 1267-1287.
717 Jung, S.W., Shin, M.H., Jung, J.H., Kim, N.D., Im, K.S.J.A.o.p.r., 2001. A triterpene glucosyl
718 ester from the roots ofRubus crataegifolius. 24, 412.
719 Kannan, N., Guruvayoorappan, C., 2013. Protective effect of Bauhinia tomentosa on acetic
720 acid induced ulcerative colitis by regulating antioxidant and inflammatory mediators.
721 International immunopharmacology 16, 57-66.
722 Keser, S., Çelik, S., Turkoglu, S., YILMAZ, Ö., Turkoglu, I., 2015. Antioxidant Properties of
723 Rubus discolor L. Extracts and Protective Effects of Its Flower Extract Against
724 Hydrogen Peroxide-Induced Oxidative Stress in Wistar Rats. Turkish Journal of
725 Pharmaceutical Sciences 12.
726 Kim, C.R., Choi, S.J., Oh, S.S., Kwon, Y.K., Lee, N.Y., Park, G.G., Kim, Y.-J., Heo, H.J.,
727 Jun, W.J., Park, C.-S., 2013. Rubus coreanus Miquel inhibits acetylcholinesterase

activity and prevents cognitive impairment in a mouse model of dementia. Journal of medicinal food 16, 785-792.
Kruidenier, L.a., Verspaget, H., 2002. oxidative stress as a pathogenic factor in inflammatory bowel disease—radicals or ridiculous? Alimentary pharmacology & therapeutics 16, 1997-2015.
Lee, J., Dossett, M., Finn, C.E., 2012. Rubus fruit phenolic research: the good, the bad, and the confusing. Food Chemistry 130, 785-796.
Li, Q., He, S., Chen, Y., Feng, F., Qu, W., Sun, H., 2018. Donepezil-based multi-functional cholinesterase inhibitors for treatment of Alzheimer's disease. European Journal of Medicinal Chemistry 158, 463-477.
Lobo, V., Patil, A., Phatak, A., Chandra, N., 2010. Free radicals, antioxidants and functional foods: Impact on human health. Pharmacognosy reviews 4, 118.
Locatelli, M., Ferrante, C., Carradori, S., Secci, D., Leporini, L., Chiavaroli, A., Leone, S., Recinella, L., Orlando, G., Martinotti, S., 2017. Optimization of aqueous extraction and biological activity of Harpagophytum procumbens root on ex vivo rat colon inflammatory model. Phytotherapy Research 31, 937-944.
Menghini, L., Ferrante, C., Leporini, L., Recinella, L., Chiavaroli, A., Leone, S., Pintore, G., Vacca, M., Orlando, G., Brunetti, L., 2016. An hydroalcoholic chamomile extract modulates inflammatory and immune response in HT29 cells and isolated rat colon. Phytotherapy Research 30, 1513-1518.
Menghini, L., Leporini, L., Vecchiotti, G., Locatelli, M., Carradori, S., Ferrante, C., Zengin, G., Recinella, L., Chiavaroli, A., Leone, S., 2018. Crocus sativus L. stigmas and byproducts: Qualitative fingerprint, antioxidant potentials and enzyme inhibitory activities. Food Research International 109, 91-98.
Mihara, M., Uchiyama, M., Fukuzawa, K., 1980. Thiobarbituric acid value on fresh homogenate of rat as a parameter of lipid peroxidation in aging, CCl4 intoxication, and vitamin E deficiency. Biochemical medicine 23, 302-311.
Mousavizadeh, K., Rahimian, R., Fakhfouri, G., Aslani, F., Ghafourifar, P., 2009. Anti-inflammatory effects of 5-HT3 receptor antagonist, tropisetron on experimental colitis in rats. European journal of clinical investigation 39, 375-383.
Nagarjun, S., Dhadde, S.B., Veerapur, V.P., Thippeswamy, B., Chandakavathe, B.N., 2017. Ameliorative effect of chromium-D-phenylalanine complex on indomethacin-induced inflammatory bowel disease in rats. Biomedicine & Pharmacotherapy 89, 1061-1066.
Ohikhena, F.U., Wintola, O.A., Afolayan, A.J., 2016. Research Article Toxicity Assessment of Different Solvent Extracts of the Medicinal Plant, Phragmanthera capitata (Sprengel) Balle on Brine Shrimp (Artemia salina).
Oliveira, B.D.Á., Rodrigues, A.C., Cardoso, B.M.I., Ramos, A.L.C.C., Bertoldi, M.C., Taylor, J.G., Cunha, L.R.d., Pinto, U.M., 2016. Antioxidant, antimicrobial and anti-quorum sensing activities of Rubus rosaefolius phenolic extract. Industrial Crops and Products 84, 59-66.
Oszmiański, J., Wojdyło, A., Nowicka, P., Teleszko, M., Cebulak, T., Wolanin, M.J.M., 2015. Determination of phenolic compounds and antioxidant activity in leaves from wild Rubus L. species. 20, 4951-4966.
Papaioanou, M., Chronopoulou, E.G., Ciobotari, G., Efrose, R.C., Sfichi-Duke, L., Chatzikonstantinou, M., Pappa, E., Ganopoulos, I., Madesis, P., Nianiou-Obeidat, I., 2018. Cosmeceutical Properties of Two Cultivars of Red Raspberry Grown under Different Conditions. Cosmetics 5, 20.
Raihan, S.Z., Chowdhury, A.A., Rabbani, G.H., Marni, F., Ali, M.S., Nahar, L., Sarker, S.D., 2009. Effect of aqueous extracts of black and green teas in arsenic-induced toxicity in rabbits. Phytotherapy research 23, 1603-1608.

778 Regmi, S.C., Park, S.-Y., Ku, S.K., Kim, J.-A., 2014. Serotonin regulates innate immune
779 responses of colon epithelial cells through Nox2-derived reactive oxygen species. Free
780 Radical Biology and Medicine 69, 377-389.
781 Ryu, J., Kim, W.J., Im, J., Kim, S.H., Lee, K.-S., Jo, H.-J., Kim, E.-Y., Kang, S.-Y., Lee, J.-
782 H., Ha, B.-K., 2018. Genotyping-by-sequencing based single nucleotide
783 polymorphisms enabled Kompetitive Allele Specific PCR marker development in
784 mutant Rubus genotypes. Electronic Journal of Biotechnology 35, 57-62.
785 Saijo, F., Milsom, A.B., Bryan, N.S., Bauer, S.M., Vowinkel, T., Ivanovic, M., Andry, C.,
786 Granger, D.N., Rodriguez, J., Feelisch, M., 2010. On the dynamics of nitrite, nitrate
787 and other biomarkers of nitric oxide production in inflammatory bowel disease. Nitric
788 Oxide 22, 155-167.
789 Sandjo, L.P., Nascimento, M.V.d.S., da Silva, L.A., Munhoz, A.C., Pollo, L.A., Biavatti,
790 M.W., Ngadjui, B.T., Opatz, T., Fröde, T.S.J.P.A., 2017. ESI-MS2 and Anti-
791 inflammatory Studies of Cyclopropanic Triterpenes. UPLC-ESI-MS and MS2 Search
792 of Related Metabolites from Donella ubanguiensis. 28, 27-41.
793 Shin JS, Cho EJ, Choi HE, Seo JH, An HJ, Park HJ, Cho YW, Lee KT. Anti-inflammatory
794 effect of a standardized triterpenoid-rich fraction isolated from Rubus coreanus on
795 dextran sodium sulfate-induced acute colitis in mice and LPS-induced macrophages. J
796 Ethnopharmacol. 2014 Dec 2;158 Pt A:291-300.
797 Soliman, N., Keshk, W., Rizk, F., Ibrahim, M., 2019. The possible ameliorative effect of
798 simvastatin versus sulfasalazine on acetic acid induced ulcerative colitis in adult rats.
799 Chemico-biological interactions 298, 57-65.
800 Spínola, V., Pinto, J., Llorent-Martínez, E.J., Tomás, H., Castilho, P.C., 2019. Evaluation of
801 Rubus grandifolius L. (wild blackberries) activities targeting management of type-2
802 diabetes and obesity using in vitro models. Food and Chemical Toxicology 123, 443-
803 452.
804 Süntar, I., Koca, U., Keleş, H., Akkol, E.K., 2011. Wound healing activity of Rubus sanctus
805 Schreber (Rosaceae): preclinical study in animal models. Evidence-Based
806 Complementary and Alternative Medicine 2011.
807 Uttara, B., Singh, A.V., Zamboni, P., Mahajan, R., 2009. Oxidative stress and
808 neurodegenerative diseases: a review of upstream and downstream antioxidant
809 therapeutic options. Current neuropharmacology 7, 65-74.
810 Uysal, A., Ozer, O.Y., Zengin, G., Stefanucci, A., Mollica, A., Picot-Allain, C.M.N.,
811 Mahomoodally, M.F., 2018. Multifunctional approaches to provide potential
812 pharmacophores for the pharmacy shelf: Heracleum sphondylium L. subsp. ternatum
813 (Velen.) Brummitt. Computational Biology and Chemistry.
814 Uysal, S., Zengin, G., Locatelli, M., Bahadori, M.B., Mocan, A., Bellagamba, G., De Luca,
815 E., Mollica, A., Aktumsek, A., 2017. Cytotoxic and enzyme inhibitory potential of two
816 Potentilla species (P. speciosa L. and P. reptans Willd.) and their chemical
817 composition. Frontiers in pharmacology 8, 290.
818 Veličković, I.Z., Grujić, S.M., Marin, P.D., 2016. Antioxidant properties of Rubus discolor
819 leaf extracts. Matica Srpska Journal for Natural Sciences.
820 Venskutonis, P.R., Dvaranauskaite, A., Labokas, J., 2007. Radical scavenging activity and
821 composition of raspberry (Rubus idaeus) leaves from different locations in Lithuania.
822 Fitoterapia 78, 162-165.
823 Verma, R., Gangrade, T., Punasiya, R., Ghulaxe, C., 2014. Rubus fruticosus (blackberry) use
824 as an herbal medicine. Pharmacognosy Reviews 8, 101-104.
825 Xu, Y., Li, L.-Z., Cong, Q., Wang, W., Qi, X.-L., Peng, Y., Song, S.-J., 2017. Bioactive
826 lignans and flavones with in vitro antioxidant and neuroprotective properties from
827 Rubus idaeus rhizome. Journal of Functional Foods 32, 160-169.

828 Zengin, G., Aktumsek, A., Ceylan, R., Uysal, S., Mocan, A., Guler, G.O., Mahomoodally,
829 M.F., Glamoclija, J., Ciric, A., Sokovic, M., 2017. Shedding light on the biological
830 and chemical fingerprints of three Achillea species (A. biebersteinii, A. millefolium
831 and A. teretifolia). Food & function 8, 1152-1165.
832 Zengin, G., Rodrigues, M.J., Abdallah, H.H., Custodio, L., Stefanucci, A., Aumeeruddy,
833 M.Z., Mollica, A., Rengasamy, K.R.R., Mahomoodally, M.F., 2018. Combination of
834 phenolic profiles, pharmacological properties and in silico studies to provide new
835 insights on Silene salsuginea from Turkey. Computational Biology and Chemistry 77,
836 178-186.
837 Zheleva-Dimitrova, D., Zengin, G., Balabanova, V., Voynikov, Y., Lozanov, V., Lazarova, I.,
838 Gevrenova, R.J.J.o.p., analysis, b., 2018. Chemical characterization with in vitro
839 biological activities of Gypsophila species. 155, 56-69.
840 Zheleva-Dimitrova, D., Gevrenova, R., Zaharieva, M.M., Najdenski, H., Ruseva, S., Lozanov,
841 V., Balabanova, V., Yagi, S., Momekov, G., Mitev, V.J.P.A., 2017. HPLC-UV and
842 LC–MS Analyses of Acylquinic Acids in Geigeria alata (DC) Oliv. & Hiern. and their
843 Contribution to Antioxidant and Antimicrobial Capacity. 28, 176-184.
844
845
846
847 **Figure legends**
848
849 Figure 1: Statistical Evaluation (**A:** Relationship between total bioactive compounds and
850 biological activities; **B:** Clustering of extracts in according to biological activities and total
851 bioactive components based on Heatmap; **C:** sPLS-DA results obtained from biologicals
852 activities of the tested extracts; **D:** Influence of 13 variables (total bioactive components and
853 biologicals activities) for the total map (VIP variable importance in the prediction).

854 Figure 2: Effect of MeOH, water and EA extracts (100 µg/mL) of *R. ibericus* and *R. sanctus*
855 on spontaneous HCT116 cell migration (wound healing test). Data are means ± SD of three
856 experiments performed in triplicate. ANOVA, $P<0.05$; post-hoc, *$P<0.05$ vs. CTR48.

857 Figure 3: Effect of MeOH, water and EA extracts (100 µg/mL) of *R. ibericus* and *R. sanctus*
858 on LPS-induced nitrite level (mmoL/g wet tissue) in rat colon specimens (N=5 per group).
859 ANOVA, $P<0.0001$; post-hoc, ***$P<0.001$ vs. LPS.

860 Figure 4: Effect of MeOH, water and EA extracts (100 µg/mL) of *R. ibericus* and *R. sanctus*
861 on LPS-induced malondialdehyde (MDA) production in rat colon tissues challenged with LPS
862 (N=5 per group). ANOVA, $P<0.001$; post-hoc, **$P<0.01$ vs. LPS.

863 Figure 5: Effect of MeOH, water and EA extracts (100 µg/mL) of *R. ibericus* and *R. sanctus*
864 on LPS-induced lactate dehydrogenase (LDH) activity in rat colon specimens (N=5 per
865 group). ANOVA, $P<0.001$; post-hoc, **$P<0.01$, ***$P<0.001$ vs. LPS.

Figure 6: Effect of MeOH, water and EA extracts (100 µg/mL) of *R. ibericus* and *R. sanctus* on serotonin (5-HT) level (ng/mg wet tissue) in rat colon specimens challenged with LPS (N=5 per group). ANOVA, P<0.001; post-hoc, **P<0.01, ***P<0.001 vs. LPS.

Table 1. Total phenolic and flavonoid contents of *Rubus sanctus* and *R. ibericus* extracts.

Extract	Total phenolic content (mg GAE/g extract)	Total flavonoid content (mg RE/g extract)
R. sanctus-EA	17.22±1.21^{e}	25.70±0.62^{d}
R. sanctus -MeOH	83.31±2.75^{d}	29.12±0.59^{c}
R. sanctus -Water	134.53±2.45^{b}	35.40±3.99^{b}
R. ibericus-EA	21.57±0.50^{e}	40.52±0.50^{a}
R. ibericus -MeOH	115.53±3.88^{c}	27.88±0.20^{cd}
R. ibericus -Water	152.55±1.45^{a}	38.08±0.23^{ab}

Values expressed are means ± S.D. of three parallel measurements. GAE: Gallic acid equivalent; RE: Rutin equivalent; EA: Ethyl acetate; MeOH: Methanol. Different superscripts indicate differences among the extracts (p<0.05).

907
908
909
910
911
912

913 Table 2. Metabolites detected in the extracts from *Rubus ibericus* and *R. sanctus*
914

Peak №	Accurate mass $[M-H]^-$ *m/z*	Molecular formula $[M-H]^-$	MS/MS data *m/z*	t_R[1(4)] min	Exact mass $[M-H]^-$ *m/z*	Delta ppm	Tentative assignment	Reference Standard (RS)/Reference
Hydroxybenzoic and hydroxycinnamic acids and derivatives								
1	331.0672	$C_{13}H_{15}O_{10}$	331.0672 (100), 169.0132 (53.31), 151.0023 (16.51), 125.0230 (20.67)	0.99	331.0659	0.303	Gallic acid-*O*-hexoside[1,2,3,4,5,6]	
2	169.0132	$C_7H_5O_5$	169.0132 (31.85), 125.0230 (100)	1.18	169.0131	-6.133	Gallic acid[1,2,3,4,5,6]	RS
3	315.0724	$C_{13}H_{15}O_9$	315.0727 (36.24), 153.0183 (100), 123.0439 (2.15), 109.0281 (44.28)	1.91	315.0710	0.935	Protocatechuic acid-*O*-hexoside[1,2,3,4,5,6]	
4	153.0182	$C_7H_5O_4$	153.0188 (11.57), 109.0281 (100), 123.0439 (85.33)	2.24	153.0182	-7.659	Protocatechuic acid[1,2,3,4,5,6]	RS
5	341.0881	$C_{15}H_{17}O_9$	341.0881 (21.0), 323.0789 (21.0), 281.0667 (100), 251.0561(55.1), 221.0452 (48.8), 179.0341 (95.6), 161.0234 (68.63), 135.0439 (68.9)	2.91	341.0867	0.813	Caffeic acid-*O*-hexoside[1,2,3,4,5,6]	Clifford et al., 2007
6	163.0390	$C_9H_7O_3$	163.0390 (23.64), 135.0438 (9.15), 119.0489 (100)	3.10	163.0389	-6.731	*p*-Coumaric acid[1,2,3,4,5,6]	RS
7	341.0887	$C_{15}H_{17}O_9$	341.0887 (21.9), 281.0667 (3.0), 251.0560 (62.1), 221.0453 (50.4), 179.0341 (100), 161.0234 (65.9), 135.0439 (72.3)	3.26	341.0867	2.770	Caffeic acid-*O*-hexoside isomer[1,2,3,4,5,6]	Clifford et al., 2007
8	179.0341	$C_9H_7O_4$	179.0341 (17.47), 135.0439 (100)	3.72	179.0338	-5.150	Caffeic acid[1,2,4,5]	RS
9	153.0182	$C_7H_5O_4$	153.0182 (65.10), 135.0074 (28.61), 122.0362 (1.56), 109.0281 (100)	4.03	153.0182	-7.463	Gentisic acid[1,2,3,4,5,6]	RS
10	503.1440	$C_{21}H_{27}O_{14}$	503.1548 (48.8), 341.0902 (3.6), 323.0787 (21.6), 179.0344 (34.3), 161.0234 (100), 135.0437 (39.4)	6.29	503.1406	6.701	Caffeoyldihexoside[4,5]	Oszmiański et al., 2015
11	504.1273	$C_{24}H_{24}O_{12}$	504.1234 (96.7), 342.0916 (18.0), 282.0702 (29.2), 252.0595 (20.7), 222.0487 (10.8), 179.0342 (46.9), 161.0234 (100), 135.0439 (45.7)	6.29	504.1234	-6.677	Dicaffeoyl-hexoside[1,2]	
12	163.0391	$C_9H_7O_3$	163.0390 (21.22), 135.0438 (4.12), 119.0489 (100)	7.04	163.0389	-6.056	*m*-Coumaric acid[4,5]	RS
Ellagitannins and ellagic acid derivatives								
13	1401.5967	$C_{66}H_{97}O_{32}$	1401.5967 (72.0), 897.0446 (7.7), 633.0735 (12.2), 300.9989 (100), 229.0138 (8.6)	4.34	1401.5968	-0.117	Ellagitannins (Lambertianin C)[4]	Oszmiański et al., 2015
14	934.0726	$C_{41}H_{26}O_{26}$	934.0726 (39.8), 663.0733 (6.6), 300.9989 (100), 257.0090 (3.9), 245.0092 (2.8), 229.0137 (6.1), 217.0136 (1.5)	4.55	934.0718	0.847	Galloyl-bis-hexahydroxyphenoyl-hexoside[1,2,3,4,5,6]	Donno et al., 2013
15	433.0415	$C_{19}H_{13}O_{12}$	433.0415 (100), 300.9990 (82.7), 257.0091 (1.3), 229.0142 (1.9)	4.76	433.0412	0.510	Ellagic acid-pentoside[1,2,3,4,5,6]	Oszmiański et al., 2015
16	447.0571	$C_{20}H_{15}O_{12}$	447.0571 (82.7), 300.994 (47.7), 299.9912 (100)	4.95	477.0569	0.382	Ellagic acid-deoxyhexoside[4]	Oszmiański et al., 2015
17	300.9991	$C_{14}H_6O_8$	300.9991 (100), 257.0092 (0.4), 245.0091 (2.3), 229.0140 (3.2), 217.0131 (0.6), 145.0281 (3.4), 117.0317 (1.3)	5.10	300.9990	0.396	Ellagic acid[1,2,3,4,5,6]	RS
Acylquinic acids								

18	353.0880	$C_{16}H_{17}O_9$	353.0880 (46.2), 191.0553 (100), 179.0342 (67.3), 173.0447 (2.0), 161.0235 (4.6), 135.0439 (50.5), 93.0331 (2.0)	2.48	353.0867	0.580	Neochlorogenic (3-caffeoylquinic) acid[1,2,3,4,5,6]	RS
19	337.0932	$C_{16}H_{17}O_8$	337.0932 (7.7), 191.0552 (7.6), 173.0443 (4.1), 163.0390 (100), 119.0489 (28.0), 93.0329 (2.7)	3.12	337.0929	0.829	3-coumaroyl-quinic acid[1,2,3,4,5,6]	Clifford et al., 2005
20	353.0881	$C_{16}H_{17}O_9$	353.0881 (6.0), 191.0554 (100), 179.0345 (3.1), 173.0450 (2.5), 161.0234 (2.3), 111.0433 (1.1), 97.4881 (0.7), 93.0331 (3.1), 127.0389 (1.7), 135.0439 (2.6)	3.29	353.0867	0.920	Chlorogenic (5-caffeoylquinic) acid[1,2,3,4,5,6]	RS
21	353.0881	$C_{16}H_{17}O_9$	353.0881 (28.3)191.0554 (56.1), 179.0341 (64.6), 173.0446 (100), 161.0229 (3.8), 135.0439 (58.8), 111.0438 (3.2), 93.0331 (21.8)	3.47	353.0867	0.920	4-caffeoylquinic acid[1,2,3,4,4,5,6]	Clifford et al., 2005
22	367.1035	$C_{17}H_{19}O_9$	367.1035 (14.7), 193.0499 (100), 173.0448 (5.3), 149.0593 (2.4), 134.0361 (58.6), 93.0331 (2.6)	3.53	367.1035	0.094	3-feruloylquinic acid[1,2,3,4,5,6]	Clifford et al., 2005
23	367.1038	$C_{17}H_{19}O_9$	367.1038 (41.0), 193.0499 (16.1), 173.0444 (2.6), 161.0233 (100), 134.0362 (9.1), 127.0388 (1.5), 85.0280 (12.4)	3.94	367.1035	0.830	1-feruloylquinic acid[1,4]	Clifford et al., 2005
24	337.0929	$C_{16}H_{17}O_8$	337.0929 (7.3), 191.0555 (0.5), 173.0446 (100), 163.0390 (20.0), 119.0400 (7.3), 93.0331 (19.1), 97.4970 (0.7)	4.12	337.0929	0.473	4-coumaroyl-quinic acid[1,2,3,4,5,6]	Clifford et al., 2005
25	337.0939	$C_{16}H_{17}O_8$	337.0939 (8.6), 191.0554 (100), 173.0444 (15.9), 163.0393 (6.4), 119.0489 (6.2), 93.0330 (20.1)	4.14	337.0929	4.532	5-coumaroyl-quinic acid[4,5]	Clifford et al., 2005
26	367.1038	$C_{17}H_{19}O_9$	367.1038 (13.7), 193.0500 (18.0), 191.0552 (5.7), 173.0446 (100), 161.0230 (3.83), 134.0361 (14.8), 111.0439 (2.4), 93.0331 (24.2)	4.50	367.1034	-1.840	4-feruloylquinic acid[1,2,3,4,5,6]	Clifford et al., 2005
27	367.1034	$C_{17}H_{19}O_9$	367.1034 (62.8), 193.0501 (0.7), 173.0445 (3.80), 161.0.234 (100), 134.0327 (1.0), 127.0388 (2.5), 111.0438 (0.4), 93.0332 (2.5), 85.0280 (17.0)	4.65	367.1034	-0.260	5-feruloylquinic acid[1,4]	Clifford et al., 2005
28	515.1198	$C_{25}H_{23}O_{12}$	515.1198 (100), 353.0883 (17.8), 335.0774 (8.2), 203.0335 (0.5), 191.0554 (41.55), 179.0341 (67.0), 173.0447 (78.8), 161.0234 (24.8), 135.0439 (67.8), 111.0436 (1.7), 93.0331 (19.8)	5.78	515.1184	0.487	3,4-dicaffeoylquinic acid[1,2,3,4,5,6]	Clifford et al., 2005
29	515.1199	$C_{25}H_{23}O_{12}$	515.1199 (13.8), 353.0879 (93.8), 335.0776 (0.8), 191.0553 (100), 179.0341 (49.9), 173.0477 (4.66), 161.0284 (5.50), 135.0439 (50.3), 111.0438 (1.64), 93.0331 (3.7), 85.0279 (8.0)	5.94	515.1184	0.720	3,5-dicaffeoylquinic acid[1,2,3,4,5,6]	Clifford et al., 2005
30	515.1196	$C_{25}H_{23}O_{12}$	515.1196 (6.3), 353.0880 (48.9), 335.0781 (1.1), 191.0554 (38.2), 179.0341 (68.5), 173.0446 (100), 161.0235 (6.0), 135.0439 (65.6), 11.0437 (1.2), 93.0331 (23.7), 85.0279 (6.2)	6.32	515.1184	0.254	4,5-dicaffeoylquinic acid[1,2,3,4,5,6]	Clifford et al., 2005
31	529.1354	$C_{26}H_{25}O_{12}$	529.1354 (7.2), 367.1035 (86.1), 193.0500 (100), 161.0236 (77.7), 134.0361 (63.3),	6.92	529.1351	0.549	3-feruloyl-5- caffeoylquinic acid[1,2]	Clifford et al., 2005
32	529.1350	$C_{26}H_{25}O_{12}$	529.1350 (74.0), 367.1030 (64.4), 193.0503(17.9), 173.0448(100), 134.0362 (14.8), 111.0439 (4.2), 93.0332 (24.5)	7.26	529.1351	-0.263	4-feruloyl-5- caffeoylquinic acid[1,2]	Clifford et al., 2005
33	529.1357	$C_{26}H_{25}O_{12}$	529.1357 (7.2), 367.1032 (20.3), 349.0930 (2.8), 191.1402 (1.8), 161.0234 (100), 134.0355 (2.0), 93.0329 (1.7)	7.32	529.1351	1.003	1-caffeoyl-5-feruloylquinic acid[1,4]	Clifford et al., 2005

34	529.1357	$C_{26}H_{25}O_{12}$	529.1357 (77.1), 367.1054 (18.6), 191.0249 (2.2), 179.0339 (62.8), 161.0233 (53.8), 134.0366 (7.1), 135.0439 (100)	7.69	529.1351	1.116	3-caffeoyl-5-feruloylquinic acid[1,4]	Clifford et al., 2005
35	677.1513	$C_{34}H_{29}O_{15}$	677.1513 (97.6), 515.1188 (44.4), 353.0874 (52.6), 335.0780 (15.4), 229.5099 (4.0), 191.0552 (51.5), 179.0341 (75.6), 173.0447 (93.7), 161.0234 (28.5), 135.0440 (100), 111.0435 (5.0), 93.0330 (24.5)	7.86	677.1512	0.172	3,4,5-tricaffeoylquinic acid[1,2]	Clifford et al., 2007
			Flavonoids					
36	609.1476	$C_{27}H_{29}O_{16}$	609.1476 (2.5), 447.0934 (28.7), 285.0409 (65.8), 255.0296 (56.5)	3.89	609.1461	2.515	Luteolin-*O*-dihexoside[1,4]	Ferreres et al., 2007
37	6091467	$C_{27}H_{29}O_{16}$	609.1467 (97.6), 429.0856 (1.0), 285.0400 (51.9), 284.0327 (100), 255.0302 (58.7), 227.0346 (34.2), 163.0029 (1.4), 151.0027 (2.0), 107.0122 (1.5)	4.87	609.1461	0.923	Kaempferol-*O*-dihexoside[1,3,4,5,6]	Ferreres et al., 2007
38	609.1462	$C_{27}H_{29}O_{16}$	609.1462 (100), 301.0349 (49.5), 300.0276 (87.9), 271.0247 (51.8), 255.0296 (22.1), 243.0293 (12.6), 227.0347 (1.6), 163.0028 (1.7), 151.0026 (8.6), 107.0125 (1.9)	5.14	609.1461	0.118	Quercetin-3-*O*-rutinoside (rutin) [1,2,3,4,5,6]	RS
39	463.0885	$C_{21}H_{19}O_{12}$	463.0885 (100), 301.0349 (53.2), 300.0277 (98.2), 271.0249 (56.4), 255.0297 (21.5), 243.0298 (11.2), 227.0344 (4.4), 151.0025 (9.9), 135.0070 (0.7), 107.0119 (2.0)	5.27	….	0.585	Quercetin-3-*O*-galactoside (Hyperoside)[1,2,3,4,5,6]	RS
40	579.1359	$C_{26}H_{27}O_{15}$	579.1359 (84.6), 429.0829 (1.4), 327.0502 (0.3), 309.0408 (0.5), 285.0398 (42.9), 284.0327 (100), 255.0296 (61.3), 227.0346 (40.3), 229.0503 (4.0), 211.0398 (2.2), 178.9976 (2.0), 163.0024 (1.4), 151.0024 (2.6), 135.0073 (1.4), 107.0124 (2.5)	5.28	579.1355	0.547	Kaempferol-2"-*O*-pentosylhexoside[1,2,3,4,5,6]	Ferreres et al., 2007
41	477.0669	$C_{21}H_{17}O_{13}$	477.0669 (54.6), 301.0356 (100), 271.0251 (1.0), 255.0300 (4.2), 243.0296 (0.9), 227.0341 (2.3), 211.0392 (2.6), 178.9978 (9.2), 163.0026 (4.3), 151.0023 (25.4), 135.0072 (0.3), 121.0281 (7.0), 107.0124 (9.9)	5.33	477.0675	-1.203	Quercetin-*O*-hexuronide[1,2,3,4,5,6]	Oszmiański et al., 2015
42	463.0882	$C_{21}H_{19}O_{12}$	463.0882 (97.6), 301.0348 (42.3), 300.0277 (100), 271.0249 (54.0), 255.0298 (21.4), 243.0297 (13.5), 227.0344 (3.1), 151.0025 (7.2), 147.0078 (0.2), 135.0073 (1.2), 107.0123 (3.0)	5.39	463.0882	0.002	Quercetin-3-*O*-glucoside (isoquercitrin)[1,2,3,4,5,6]	RS
43	461.0728	$C_{21}H_{17}O_{12}$	461.0728 (48.8), 357.0616 (0.8), 327.0498 (1.4), 297.0393 (0.3), 285.0406 (100), 241.0504 (1.0), 229.0515 (0.3), 217.0507 (1.3), 151.0025 (5.4), 133.0282 (11.1), 107.0124 (3.0)	5.48	461.0725	0.501	Luteolin-*O*-hexuronide[4,5,6]	de Rijke et al., 2006
44	433.0805	$C_{20}H_{17}O_{11}$	433.0805 (100), 301.0356 (58.7), 300.0272 (98.4), 271.0248 (56.5), 255.0301 (18.9), 243.0303 (13.0), 151.0027 (4.4)	5.60	433.0776		Quercetin-*O*-pentoside[1,2,3]	Oszmiański et al., 2015
45	593.1511	$C_{27}H_{29}O_{15}$	593.1511 (91.5), 285.0403 (100), 255.0300 (53.6), 229.0504 (8.4), 227.0346 (37.5), 161.0226 (1.0), 151.0023 (3.3), 135.0072 (1.0), 107.0126 (3.1)	5.74	593.1512	0.415	Kaempferol-3-*O*-rutinoside[4,5,6]	RS

46	447.0564	$C_{20}H_{15}O_{12}$	447.0564 (95.2), 315.0150 (100), 299.9913 (89.9), 270.9887 (34.7), 255.0299 (2.5), 227.0356 (1.1)	5.87	477.0569	0.110	Isorhamnetin-*O*-pentoside[1,2,3,4,5,6]	de Rijke et al., 2006
47	477.1020	$C_{22}H_{21}O_{12}$	477.1020 (100), 315.0497 (19.4), 314.0434 (60.7), 300.0272 (11.6), 299.0197 (14.4), 271.0249 (37.5), 243.0297 (24.6), 179.0340 (35.3), 161.0233 (24.4), 151.0023 (5.8), 135.0440 (29.5)	5.89	477.1038	-3.897	Isorhamnetin-3-*O*-glucoside[1,2,3,4,5,6]	RS
48	461.0732	$C_{21}H_{17}O_{12}$	461.0732 (9.5), 285.0406 (100), 257.0457 (4.1), 229.0502 (10.2), 211.0398 (2.2), 201.0548 (1.1), 151.0022 (1.1), 163.0029 (1.4), 135.0073 (1.5), 131.0492 (0.3), 107.0123 (2.8)	5.95	461.0725	1.368	Kaempferol-*O*-hexuronide[1,2,3,4,5,6]	Oszmiański et al., 2015
49	447.0938	$C_{21}H_{19}O_{11}$	447.0938 (100), 285.0327 (28.2), 284.0397 (75.1), 255.0298 (57.6), 227.0346 (58.9), 151.0025 (2.8), 135.0073 (0.57), 107.0124 (1.1)	5.96	447.0933	1.041	Kaempferol-3-*O*-glucoside[1,2,3,4,5,6]	RS
50	447.0875	$C_{21}H_{19}O_{11}$	447.0938 (100), 285.0405 (77.8), 271.0249 (14.6), 243.0304 (16.7), 227.0337 (4.1), 151.0026 (3.7), 133.0281 (9.4), 107.0121 (2.6)	6.39	447.0933	-12.894	Luteolin-7-*O*-glucoside[1,2,3,4,6]	RS
51	609.1250	$C_{30}H_{25}O_{14}$	609.1250 (100), 447.0944 (5.3), 285.0406 (84.3), 255.0299 (30.0), 229.0506 (7.4), 227.0349 (22.9), 211.0394 (1.4), 179.0340 (13.0), 161.0234 (30.3), 151.0024 (2.2), 135.0439 (18.7), 107.0123 (2.3)	7.07	609.1250	0.035	Kaempferol-*O*-caffeoylhexoside[1,2,4]	de Rijke et al., 2006
52	593.1306	$C_{30}H_{25}O_{13}$	593.1306 (100), 447.0936 (3.1), 285.0403 (82.8), 257.0457 (2.9), 255.0300 (56.4), 239.0346 (1.6), 229.0502 (6.9), 227.0347 (39.4), 211.0395 (3.30), 151.0026 (3.7), 119.0489 (3.8), 117.0332 (3.8), 107.0120 (2.9)	7.77	593.1301	0.937	Kaempferol-3-*O*-*p*-coumaroyl-glucoside (tiliroside)[1,2,3,4,5,6]	RS
53	289.0720	$C_{15}H_{13}O_6$	289.0720 (100), 245.0822 (41.2), 205.0505 (15.7), 203.0702 (18.9), 163.0383 (2.0), 137.0230 (18.0), 121.0279 (8.5)	3.99	289.0718	0.687	Epicatechin	RS
54	285.0406	$C_{15}H_9O_6$	285.0406 (100), 241.0498 (0.78), 201.0180 (0.7), 151.0025 (6.5), 133.0282 (26.5), 107.0124 (4.8)	7.69	285.0405	0.452	Luteolin[1,2,3,4,5,6]	RS
55	301.0360	$C_{15}H_9O_7$	301.0360 (100), 273.0412 (3.9), 255.0297 (3.5), 229.0499 (1.8), 178.9978 (25.4), 163.0027 (0.7), 151.0025 (49.5), 11.60 (121.0281 (15.2), 107.0124 (14.5)	7.70	301.0354	2.007	Quercetin[1,2,3,4,6]	RS
56	285.0404	$C_{15}H_9O_6$	285.0404 (-0.320), 239.0354 (1.0), 229.0512 (1.4), 107.0122 (1.2)	8.97	285.0405		Kaempferol[1,2,3,4,5,6]	RS
57	315.0515		315.0515 (81.4), 300.0277 (100), 301.0305 (10.5), 255.0302 (2.4), 243.0299 (1.7), 227.0351 (3.0)	8.98	315.0510	1.632	Isorhamnetin[1,2,3,4,5,6]	RS
Triterpenoid saponins								
58	711.3967	$C_{36}H_{57}O_{11}$	711.3967 (99.0), 665.3905 (13.6), 503.3378 (100), 485.3265 (2.0)	7.26	711.3961	0.865	Ilexosapogenin A-hexoside[1,2,3,4,5,6]	Jung et al., 2001
59	679.3703	$C_{36}H_{55}O_{12}$	679.3703 (100), 517.3170 (32.9), 499.3042 (0.4), 473.3264 (0.4), 455.3171 (6.7), 437.3052 (2.5), 393.3796 (0.4)(	8.26	679.3699	0.588	Barrinic acid-hexoside[1,2,3,4,5,6]	Jung et al., 2001

60	709.3809	$C_{37}H_{57}O_{13}$	709.3809 (77.8), 663.3756 (12.1), 501.3226 (100), 483.3106 (1.3), 455.3175 (0.6), 439.3161 (0.4), 437.3079 (0.5), 421.3124 (3.4)	8.36	709.3805	0.557	Hydroxygypsogenic acid-hexoside[1,2,3,4,5,6]	Jung et al., 2001
61	679.3704	$C_{36}H_{55}O_{12}$	679.3704 (100), 517.3185 (31.6), 455.3193 (3.3), 437.3068 (2.5)	8.39	679.3699	0.677	Barrinic acid-hexoside isomer[1,2,3,4,5,6]	
62	709.3809	$C_{37}H_{57}O_{13}$	709.3808 (67.7), 663.3767 (10.4), 501.3225 (100), 483.3120 (4.4)	8.59	709.3805	0.472	Hydroxygypsogenic acid-hexoside isomer[1,2,3,4,5,6]	
63	695.4022	$C_{37}H_{59}O_{12}$	695.4022 (91.9), 649.3929 (16.5), 487.3429 (100), 423.3273 (3.4)	9.10	695.4012	1.380	Arjunolic acid-hexoside[1,2,3,4,5,6]	Jung et al., 2001
64	695.4012	$C_{37}H_{59}O_{12}$	695.4022 (76.3), 649.3929 (10.5), 487.3429 (100)	9.31	695.4012	1.380	Arjunolic acid-hexoside isomer[1,2,3,4,5,6]	
65	503.3361	$C_{30}H_{47}O_6$	503.3361 (100), 485.3277 (6.7), 473.3252 (1.1), 459.3103 (12.2), 457.3341 (3.3), 441.3391 (9.1), 439.3219 (1.2), 421.3129 (3.1), 407.2959 (0.9)	11.49	503.3378	-3.482	Ilexosapogenin A[3,6]	Jung et al., 2001
66	517.3173	$C_{30}H_{45}O_7$	517.3173 (100), 499.3062 (2.6), 473.3303 (3.9), 455.3168 (11.0), 439.2848 (3.5), 421.2749 (0.6)	12.12	517.3171	0.354	Barrinic acid[3,6]	Jung et al., 2001
67	487.3430	$C_{30}H_{47}O_5$	487.3430 (100), 469.2954 (0.6), 441.2969 (2.4), 423.2913 (0.5), 407.2961 (17.2), 405.2784 (1.9), 389.2856 (.5)	13.21	487.3430	0.251	Arjunolic acid[3,6]	Jung et al., 2001
68	501.3220	$C_{30}H_{45}O_6$	501.3230 (100), 483.3107 (2.8), 471.3132 (0.5), 455.3171 (1.5), 437.3069 (1.2), 421.3119 (8.0), 419.2961 (1.9), 401.2869 (1.6), 393.3166 (0.6)	13.84	501.3222	1.731	Hydroxygypsogenic acid[3,6]	Jung et al., 2001

[1]*Rubus sanctus*-MeOH; [2]*R. sanctus*-Water; [3]*R. sanctus*-EA; [4]*R. ibericus*-MeOH; [5]*R. ibericus*-Water; [6]*R. ibericus*-EA. t_R[1(4)] retention times are referred to *Rubus sanctus* methanolic extract ([1]), *R. ibericus* methanolic extract ([4]) and *R. ibericus* ethylacetate extract ([6])

Table 3. Antioxidant activities of *Rubus sanctus* and *R. ibericus* extracts.

Extract	DPPH (mg TE/g extract)	ABTS (mg TE/g extract)	CUPRAC (mg TE/g extract)	FRAP (mg TE/g extract)	Phosphomolybdenum (mmol TE/g)	Metal chelating ability (mg EDTAE/g)
R. sanctus-EA	24.12±0.81^{f}	28.19±2.64^{e}	71.08±6.40^{f}	26.81±2.33^{e}	1.65±0.03^{f}	46.91±2.46^{c}
R. sanctus -MeOH	347.61±13.21^{d}	279.95±11.13^{d}	456.23±5.56^{d}	245.93±5.44^{d}	2.50±0.12^{d}	39.68±2.46^{d}
R. sanctus -Water	386.39±10.97^{c}	543.68±14.28^{b}	762.96±2.95^{b}	486.85±3.24^{b}	3.05±0.04^{c}	52.20±0.19^{b}
R. ibericus-EA	37.37±0.66^{e}	34.15±4.53^{e}	91.42±1.45^{e}	32.89±2.41^{e}	1.97±0.04^{e}	47.30±1.32^{c}
R. ibericus -MeOH	487.60±0.93^{a}	483.51±7.25^{c}	681.88±5.44^{c}	416.13±14.69^{c}	3.92±0.10^{b}	53.27±0.14^{b}
R. ibericus -Water	453.74±11.99^{b}	663.40±12.58^{a}	921.92±6.85^{a}	616.63±7.12^{a}	4.52±0.06^{a}	59.83±0.52^{a}

Values expressed are means ± S.D. of three parallel measurements. TE: Trolox equivalent; EDTAE: EDTA equivalent; EA: Ethyl acetate; MeOH: Methanol. Different superscripts indicate differences among the extracts (p<0.05).

Table 4. Enzyme inhibitory properties of *Rubus sanctus* and *R. ibericus* extracts.

Extract	AChE (mg GALAE/g extract)	BChE (mg GALAE/g extract)	Tyrosinase (mg KAE/g extract)	α-amylase (mmol ACAE/g extract)	α-glucosidase (mmol ACAE/g extract)
R. sanctus-EA	2.88±0.10^{b}	2.18±0.31^{b}	121.55±2.39^{b}	0.73±0.05^{b}	23.30±1.26^{b}
R. sanctus -MeOH	3.30±0.21^{a}	1.41±0.03^{c}	131.44±0.37^{a}	0.72±0.01^{b}	na
R. sanctus -Water	na	na	78.14±3.23^{d}	0.12±0.01^{c}	24.85±0.53^{a}
R. ibericus-EA	2.28±0.04^{c}	2.49±0.24^{a}	124.28±1.04^{b}	0.82±0.06^{a}	24.67±0.04^{a}
R. ibericus -MeOH	3.20±0.05^{a}	0.27±0.04^{d}	132.05±1.57^{a}	0.67±0.04^{b}	na
R. ibericus -Water	0.25±0.06^{d}	na	83.99±2.62^{c}	0.11±0.01^{c}	na

Values expressed are means ± S.D. of three parallel measurements. GALAE: Galatamine equivalent; KAE: Kojic acid equivalent; ACAE: Acarbose equivalent; na: not active; EA: Ethyl acetate; MeOH: Methanol. Different superscripts indicate differences among the extracts (p<0.05).

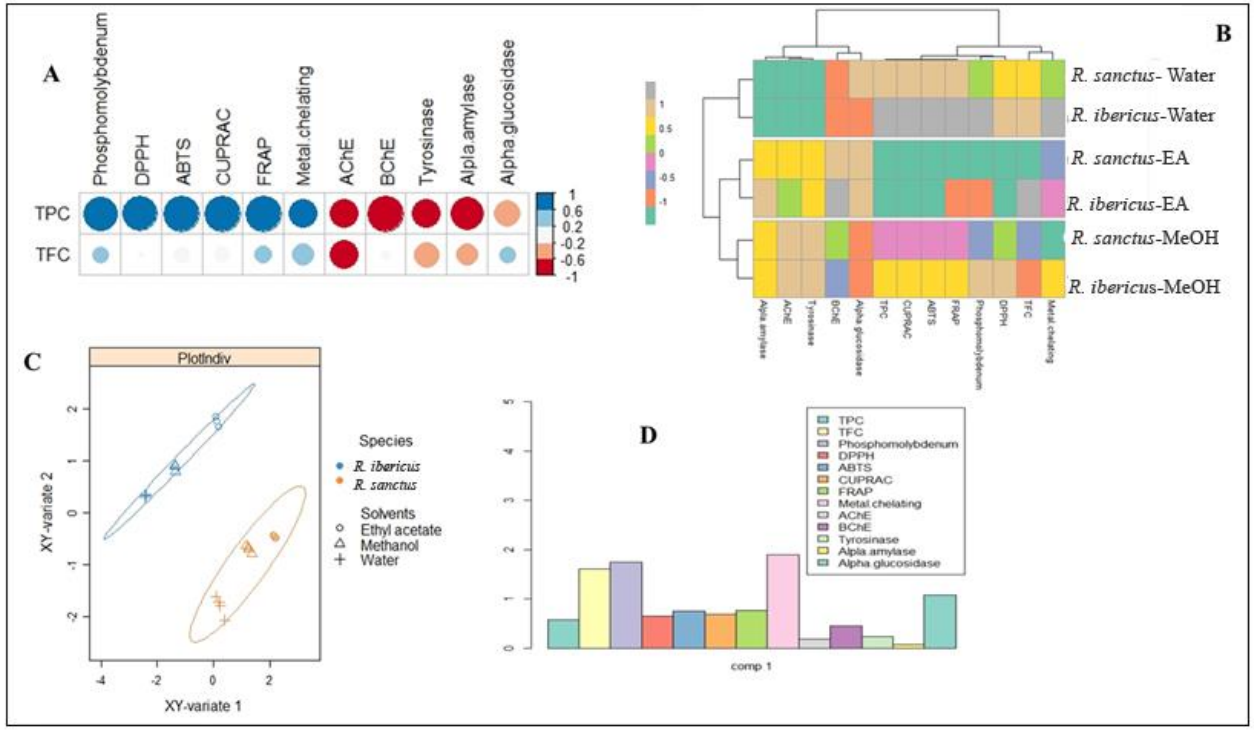

973
974 Figure 1.

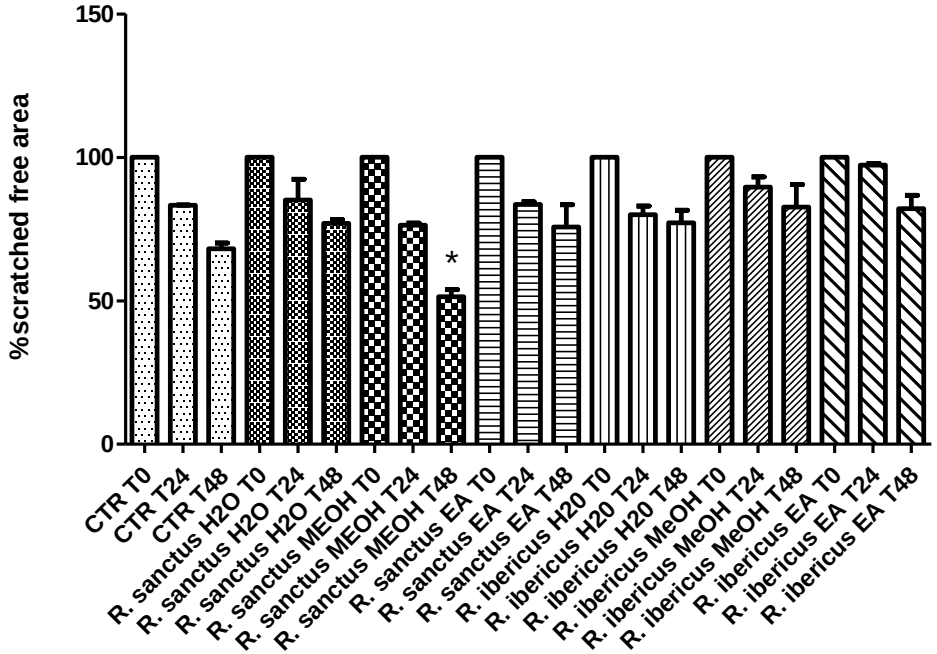
150
100
50
0
%scratched free area
*
CTR T0
CTR T24
CTR T48
R. sanctus H2O T0
R. sanctus H2O T24
R. sanctus H2O T48
R. sanctus MEOH T0
R. sanctus MEOH T24
R. sanctus MEOH T48
R. sanctus EA T0
R. sanctus EA T24
R. sanctus EA T48
R. ibericus H20 T0
R. ibericus H20 T24
R. ibericus H20 T48
R. ibericus MeOH T0
R. ibericus MeOH T24
R. ibericus MeOH T48
R. ibericus EA T0
R. ibericus EA T24
R. ibericus EA T48

Figure 2.

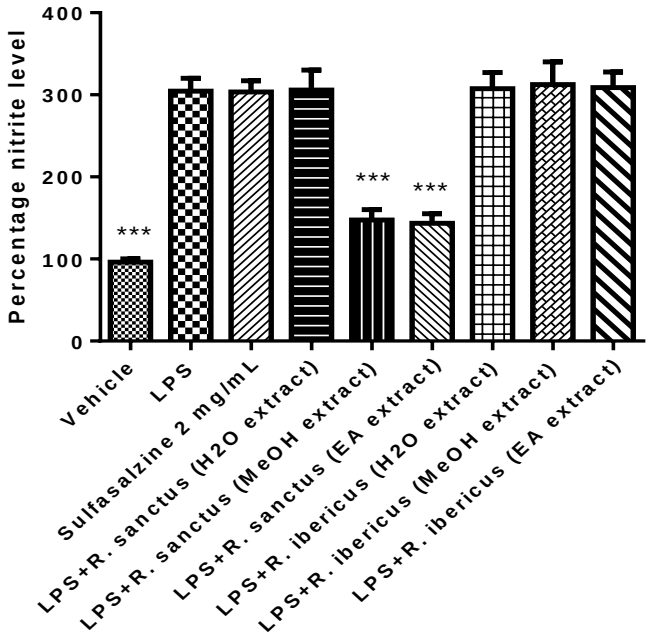
Percentage nitrite level
400
300
200
100
0
***
***
***
Vehicle
LPS
Sulfasalzine 2 mg/mL
LPS+R. sanctus (H2O extract)
LPS+R. sanctus (MeOH extract)
LPS+R. sanctus (EA extract)
LPS+R. ibericus (H2O extract)
LPS+R. ibericus (MeOH extract)
LPS+R. ibericus (EA extract)

Figure 3.

993

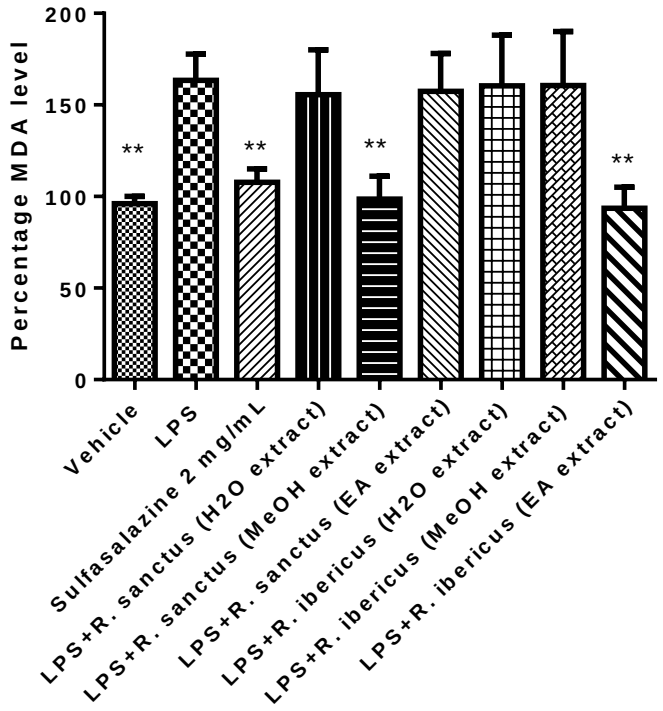

994
995 Figure 4.
996
997
998
999

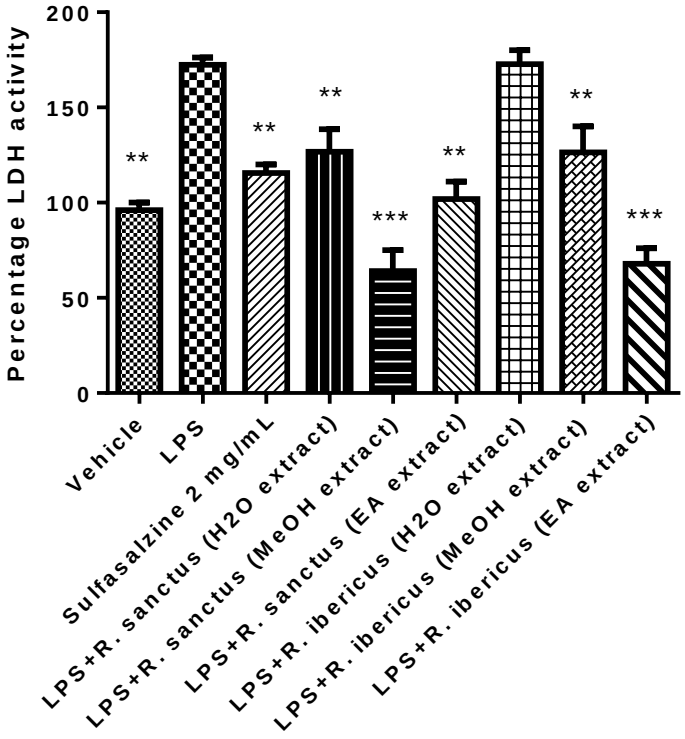
Percentage LDH activity
200
150
100
50
0
**
**
**
***
**
**
***
Vehicle
LPS
Sulfasalzine 2 mg/mL
LPS+R. sanctus (H2O extract)
LPS+R. sanctus (MeOH extract)
LPS+R. sanctus (EA extract)
LPS+R. ibericus (H2O extract)
LPS+R. ibericus (MeOH extract)
LPS+R. ibericus (EA extract)

Figure 5.

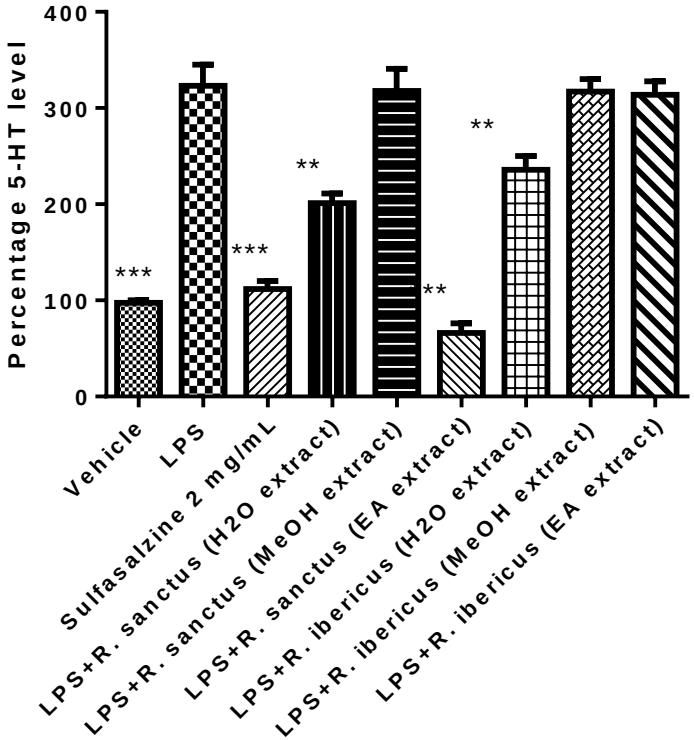
Percentage 5-HT level
400
300
200
100
0
***
***
**
**
**
Vehicle
LPS
Sulfasalzine 2 mg/mL
LPS+R. sanctus (H2O extract)
LPS+R. sanctus (MeOH extract)
LPS+R. sanctus (EA extract)
LPS+R. ibericus (H2O extract)
LPS+R. ibericus (MeOH extract)
LPS+R. ibericus (EA extract)

Figure 6.